



International Agreement Report

Assessment of RELAP5/MOD3.2.2 γ Against Flooding Database in Horizontal-to-Inclined Pipes

Prepared by
H.T. Kim, H.C. No
Korea Advanced Institute of Science and Technology
373-1, Gusung-Dong, Yuseong-Ku, Taejon 305-701 Korea

S.J. Ha, N.S. Ahn
Korea Electric Power Research Institute
103-16 Munji-Dong, Yuseong-Ku, Taejon 305-380 Korea

Y.S. Bang
Korea Institute of Nuclear Safety
PO Box 114, Yuseong-Gu, Taejon 305-600 Korea

Office of Nuclear Regulatory Research
U.S. Nuclear Regulatory Commission
Washington, DC 20555-0001

July 2001

Prepared as part of
The Agreement on Research Participation and Technical Exchange
under the International Code Application and Maintenance Program (CAMP)

Published by
U.S. Nuclear Regulatory Commission

AVAILABILITY OF REFERENCE MATERIALS IN NRC PUBLICATIONS

NRC Reference Material

As of November 1999, you may electronically access NUREG-series publications and other NRC records at NRC's Public Electronic Reading Room at www.nrc.gov/NRC/ADAMS/index.html.

Publicly released records include, to name a few, NUREG-series publications; *Federal Register* notices; applicant, licensee, and vendor documents and correspondence; NRC correspondence and internal memoranda; bulletins and information notices; inspection and investigative reports; licensee event reports; and Commission papers and their attachments.

NRC publications in the NUREG series, NRC regulations, and *Title 10, Energy*, in the Code of *Federal Regulations* may also be purchased from one of these two sources.

1. The Superintendent of Documents
U.S. Government Printing Office
Mail Stop SSOP
Washington, DC 20402-0001
Internet: bookstore.gpo.gov
Telephone: 202-512-1800
Fax: 202-512-2250
2. The National Technical Information Service
Springfield, VA 22161-0002
www.ntis.gov
1-800-553-6847 or, locally, 703-605-6000

A single copy of each NRC draft report for comment is available free, to the extent of supply, upon written request as follows:

Address: Office of the Chief Information Officer,
Reproduction and Distribution
Services Section

U.S. Nuclear Regulatory Commission
Washington, DC 20555-0001

E-mail: DISTRIBUTION@nrc.gov

Facsimile: 301-415-2289

Some publications in the NUREG series that are posted at NRC's Web site address www.nrc.gov/NRC/NUREGS/indexnum.html are updated periodically and may differ from the last printed version. Although references to material found on a Web site bear the date the material was accessed, the material available on the date cited may subsequently be removed from the site.

Non-NRC Reference Material

Documents available from public and special technical libraries include all open literature items, such as books, journal articles, and transactions, *Federal Register* notices, Federal and State legislation, and congressional reports. Such documents as theses, dissertations, foreign reports and translations, and non-NRC conference proceedings may be purchased from their sponsoring organization.

Copies of industry codes and standards used in a substantive manner in the NRC regulatory process are maintained at—

The NRC Technical Library
Two White Flint North
11545 Rockville Pike
Rockville, MD 20852-2738

These standards are available in the library for reference use by the public. Codes and standards are usually copyrighted and may be purchased from the originating organization or, if they are American National Standards, from—

American National Standards Institute
11 West 42nd Street
New York, NY 10036-8002
www.ansi.org
212-642-4900

Legally binding regulatory requirements are stated only in laws; NRC regulations; licenses, including technical specifications; or orders, not in NUREG-series publications. The views expressed in contractor-prepared publications in this series are not necessarily those of the NRC.

The NUREG series comprises (1) technical and administrative reports and books prepared by the staff (NUREG-XXXX) or agency contractors (NUREG/CR-XXXX), (2) proceedings of conferences (NUREG/CP-XXXX), (3) reports resulting from international agreements (NUREG/IA-XXXX), (4) brochures (NUREG/BR-XXXX), and (5) compilations of legal decisions and orders of the Commission and Atomic and Safety Licensing Boards and of Directors' decisions under Section 2.206 of NRC's regulations (NUREG-0750).

DISCLAIMER: This report was prepared under an international cooperative agreement for the exchange of technical information. Neither the U.S. Government nor any agency thereof, nor any employee, makes any warranty, expressed or implied, or assumes any legal liability or responsibility for any third party's use, or the results of such use, of any information, apparatus, product or process disclosed in this publication, or represents that its use by such third party would not infringe privately owned rights.

NUREG/IA-0203



International Agreement Report

Assessment of RELAP5/MOD3.2.2 γ Against Flooding Database in Horizontal-to-Inclined Pipes

Prepared by
H.T. Kim, H.C. No
Korea Advanced Institute of Science and Technology
373-1, Guseong-Dong, Yuseong-Ku, Taejeon 305-701 Korea

S.J. Ha, N.S. Ahn
Korea Electric Power Research Institute
103-16 Munji-Dong, Yuseong-Ku, Taejeon 305-380 Korea

Y.S. Bang
Korea Institute of Nuclear Safety
PO Box 114, Yuseong-Gu, Taejeon 305-600 Korea

Office of Nuclear Regulatory Research
U.S. Nuclear Regulatory Commission
Washington, DC 20555-0001

July 2001

Prepared as part of
The Agreement on Research Participation and Technical Exchange
under the International Code Application and Maintenance Program (CAMP)

Published by
U.S. Nuclear Regulatory Commission

Assessment of RELAP5/MOD3.2.2 γ Against Flooding Database in Horizontal-to-Inclined Pipes

ABSTRACT

A total of 356 experimental data for the onset of flooding are compiled for the data bank and used for the assessment of RELAP5/MOD3.2.2 γ predictions of Counter-Current Flow Limitation (CCFL) in horizontal-to-inclined pipes simulating a PWR hot leg.

RELAP5 calculations show that higher gas flow rates are required to initiate the flooding compared with the experimental data if the L/D is as low as that of the hot legs of typical PWRs.

Based on the present data bank, the new CCFL correlation is derived, which shows the L/D effect. The present correlation agrees well with the database within the prediction error, 8.7% and it is implemented into the RELAP5 and validated against the data bank.

The predictions of the flooding limit by the modified version lie well on the applied CCFL curve even if the predictions by standard RELAP5 are lower than the present CCFL curve.

Key Words: RELAP5/MOD3.2, CCFL, Flooding Database

CONTENTS

ABSTRACT	iii
CONTENTS	v
LIST OF TABLES	vii
LIST OF FIGURES	vii
SUMMARY	viii
NOMENCLATURES	ix

1. Introduction	1
2. The Flooding Database	4
2.1. Length-to-Diameter Ratio (L/D) Effect on CCFL	6
2.2. Inclination Angle (θ) of Elbow Effect on CCFL	7
2.3. Development of Empirical Flooding Correlation	8
3. RELAP5 Model	11
3.1. Code Description	11
3.2. RELAP5 Nodalization	11
3.3. Simulation Procedure	12
4. Code Calculations of the Database	15
4.1. Length-to-Diameter Ratio (L/D) Effect on RELAP5 Predictions	15
4.2. Inclination Angle (θ) of Elbow Effect on RELAP5 Predictions	16
5. Application of Empirical Flooding Correlation to RELAP5	17
5.1. Modification of RELAP5/MOD3.2.2 γ	17

5.2. Comparison of Code Calculation Results by Standard and Modified Versions	20
6. Conclusions	22
References	23
Appendix A. Sample Input Deck for CCFL Test	
Appendix B. Modification Parts in the RELAP5 Subroutines	
Appendix C. Flooding Database	

LIST OF TABLES

Table 1	Experimental Flooding Data for CCFL in Horizontal-to-Inclined Pipes	4
Table 2	Input Requirement for CCFL Data Card	17

LIST OF FIGURES

Fig. 1	General Configuration of the CCFL Test	3
Fig. 2	Experimental Flooding Points from the Present Database	5
Fig. 3	Effect of Horizontal Pipe Length-to-Diameter Ratio on CCFL	6
Fig. 4	Effect of Inclination Angle of Elbow on CCFL	7
Fig. 5	Comparison between the Present Database and Empirical Correlation	9
Fig. 6	Comparison between the Present Empirical Correlation and NO and Choi's Data	10
Fig. 7	RELAP5 Nodalization of CCFL Test in a Horizontal-to-Inclined Pipe	13
Fig. 8	Variation of Gas and Liquid Flow Rates at the Onset of CCFL	14
Fig. 9	Comparison of RELAP5 with Experimental Results with Various L/Ds	15
Fig. 10	Effect of Inclination Angle on RELAP5 Calculations	16
Fig. 11	Flow Chart of the Subroutine CCFL	18
Fig. 12	Flow Chart of the Modified Subroutine RPIPE	19
Fig. 13	Comparison of Experimental Data with Small L/D With Predictions by Standard & Modified RELAP5	21
Fig. 14	Comparison of Experimental Data with Large L/D With Predictions by Standard & Modified RELAP5	21

SUMMARY

A total of 356 experimental data for the onset of flooding are compiled for the data bank and used for the assessment of RELAP5/MOD3.2.2γ predictions of Counter-Current Flow Limitation (CCFL) in horizontal-to-inclined pipes simulating a PWR hot leg.

The predictions of the flooding gas velocity in the database are known to be largely dependent on the horizontal pipe length-to-diameter ratio (L/D). RELAP5 calculations are compared with the experimental data where L/D is varied within the range of database.

RELAP5 calculations show that the RELAP5 predicts the flooding points qualitatively well but higher gas flow rate is required to initiate the flooding compared with the experimental data if the L/D is as low as that of the hot legs of typical PWRs.

Based on the present data bank, the new CCFL correlation is derived, which shows the L/D effect. The present correlation agrees well with the database within the prediction error, 8.7%. The result of empirical correlation based on the present data bank is as follows:

$$j_g^{*0.5} + 0.614 j_f^{*0.5} = 0.635 - 0.00254 \left(\frac{L}{D} \right).$$

Standard RELAP5 code is modified to apply the present empirical CCFL curve to the horizontal volumes. The predictions of the flooding limit by the modified version lie well on the applied CCFL curve even if the predictions by standard RELAP5 are lower than the present CCFL curve.

NOMENCLATURES

- L Length of horizontal part of test section (m)
 D Diameter of test section (m)
 l Length of inclined part of test section (m)
 m Slope at Wallis type flooding correlation
 c Intercept at Wallis type flooding correlation
 g Gravitational acceleration (m/sec^2)
 La Laplace capillary constant
 w Defined in Eq. (3)
 j_k Superficial velocity for k phase (m/sec)
 j_k^* Dimensionless superficial velocity for k phase

Greek

- θ Inclination angle of test section ($^\circ$)
 ρ Density (m^3/kg)
 σ Surface tension (N/m)
 β A number from 0 to 1 in Eq. (3)

Subscript

- f For liquid phase
 g For gas phase

1. Introduction

Counter-Current Flow Limitation (CCFL) of steam and water can be observed in the hot leg during emergency core cooling following a Loss-of Coolant Accident (LOCA). When saturated water condensed in the Steam Generator (SG) tubes drains back down into the reactor vessel via the hot leg (reflux condensation cooling mode), the possibility that steam previously boiled off in the core could partly or totally inhibit the water back down flow is one of the important concerns regarding the safety analysis of the Pressurized Water Reactor (PWR).

A general CCFL model (Riemke, 1991) was implemented in RELAP5/MOD3 that allows the user to select the Wallis form, the Kutateladze form, or a form in between the Wallis and Kutateladze forms:

$$H_g^{1/2} + m H_f^{1/2} = c, \quad (1)$$

where subscript f is for liquid phase, subscript g is for gas phase, m is a slope and c is a gas intercept and the dimensionless fluxes have the form:

$$H_k = j_k \left[\frac{\rho_k}{g w (\rho_f - \rho_g)} \right]^{1/2}, \quad k = f, g \quad (2)$$

where j_k is the superficial velocity for each phase, g is a gravitational acceleration and w is given by the expression:

$$w = D^{1-\beta} L a^\beta, \quad (3)$$

where D is a junction hydraulic diameter and L is the Laplace capillary constant given by:

$$La = \left[\frac{\sigma}{g(\rho_f - \rho_g)} \right]^{1/2}, \quad (4)$$

where σ is the surface tension. In Eq. (3), β can be a number from 0 to 1. For $\beta=0$, the Wallis form of the CCFL equation is obtained, and for $\beta=1$, the Kutateladze form of CCFL equation is obtained. For $0<\beta<1$, a combination of the Wallis and Kutateladze form is obtained. The RELAP5 input is made general so that the user can input CCFL correlations for the particular geometry of interest in the volumes with the inclination angle over than 45° .

To use the CCFL curve given by user also in the horizontal volumes, NO and Heo (2000) extended the CCFL model of RELAP5 for the vertical volumes ($>45^\circ$) to the horizontal volumes and enabled the user to input the information of length-to-diameter ratio (L/D) into the gas intercept, c in Eq. (1). However, if the flooding limit by the interfacial and the wall drags are higher than that by the flooding curve, NO's model cannot be applied to the simulation of CCFL in the horizontal volumes. In the present study the interfacial and the wall drags are reduced when flooding occurs at lower gas velocity than predicted by the CCFL curve in standard RELAP5.

Through a literature survey as shown in Table 1, a data bank is constructed: 356 data in terms of dimensionless Wallis-type gas velocities and liquid velocities identified with the geometrical conditions such as horizontal pipe diameter (D), length (L) and the inclination angle (θ) of the bend. Figure 1 shows the general configuration of the CCFL test facility.

RELAP5 nodalization is developed for the simulation of the experiments in the database. To simulate the experimental results, the geometries of the horizontal-to-inclined pipes in the RELAP5 model are maintained the same as those of the experimental conditions. The parametric effects on flooding are investigated by comparing RELAP5 results with the experimental data selected from the data bank covering a wide range of the parameters.

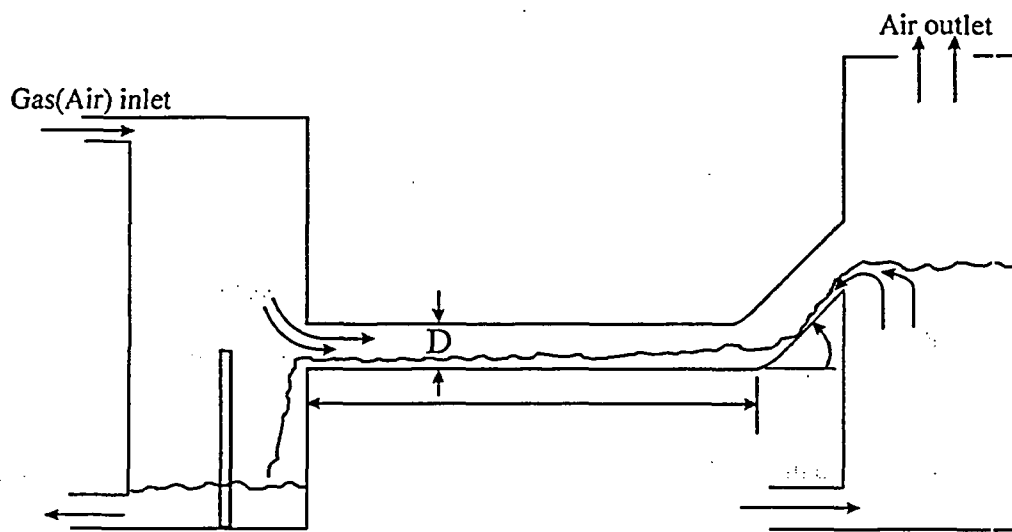


Fig. 1. General Configuration of the CCFL Test

2. The Flooding Database

From the literature survey a considerable amount of flooding data has been collected together to form a data bank containing 356 flooding points. Most of data points are the measurements of the onset of flooding limits in air-water counter-current flows in horizontal tubes connected at the water inlet to the elbows with the inclination angles from 35° to 90°. Table 1 summarizes the sources of flooding data and gives details of tube geometries and the inclination angles of bends. Figure 2 presents the flooding data points in graphical form and the dimensionless gas and liquid velocities are the dimensionless superficial velocities from the Wallis form of CCFL equation.

Table 1. Experimental Flooding Data for CCFL in Horizontal-to-Inclined Pipes

Ref.	Tube diameter range (m)	Tube length range (m)	Inclination angle of riser (θ)	Number of data points
Ohnuki (1986)	0.026, 0.076	0.01 ~ 0.4	40°, 45°	146
Wan (1986)	0.051	2.958	90°	18
Siddiqui (1986)	0.038 ~ 0.047	1.82 ~ 2.36	90°	32
Kawaji (1991)	0.051	2.54	90°	7
UPTF (1993)	0.75	7.086	50°	7
MHYRESA (1995)	0.351	2.645	50°	9
Wongwises (1996)	0.064	0.557 ~ 1.408	50° ~ 90°	104
Kang (1999)	0.04, 0.08	0.7 ~ 3.388	35°	33

In the experiments by Kawaji (1991), Wongwises (1996), and Kang (KAIST, 1999), the flooding curve is divided into three regions due to a change in the flooding mechanism. In these cases the flooding data points are confined to the first region (Wongwises, 1996), where the air flow rate that

creates the onset of flooding decreases, while the water flow rate increases. Therefore, all the flooding data points obtained are close to the widely accepted Wallis correlation.

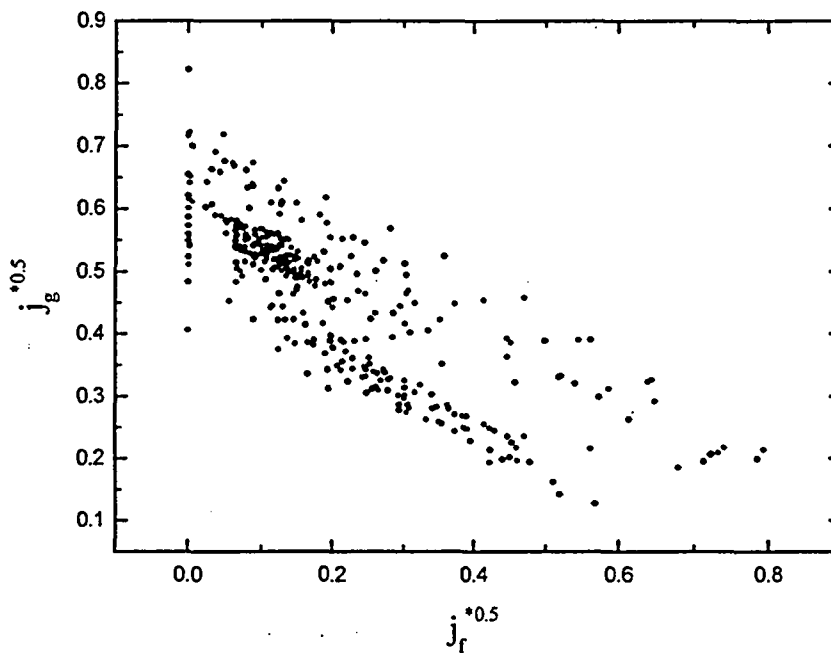


Fig. 2. Experimental Flooding Points from the Present Database

The experiments on flooding in horizontal-to-inclined pipes were conducted over different conditions, such as tube diameter (D), length (L), inclination of the elbow (θ), radius of curvature of the elbow, and inlet or exit geometry of tube. Ohnuki (1986), Siddiqui (1986), Wongwises, and Kang found that flooding limit in a horizontal-to-inclined pipe is strongly dependent on the length-to-diameter ratio (L/D) within the range of experimental tests. The effects of other parameters are not clear and inappropriate for RELAP5 code modelling except the parameter, θ .

Therefore, 2 parametric effects, L/D and θ on flooding limits are investigated in this study. And the effects of geometric parameters on CCFL are used to correlate all the data in Table 1 by the linear relationship expressed in Wallis-type correlation.

2.1. Length-to-Diameter Ratio (L/D) Effect on CCFL

Ohnuki, Siddiqui, Wongwises, and Kang performed experiments in which the length of the horizontal pipe was varied. According to their results a longer horizontal length causes the water level to be higher in the vicinity of the bend due to an increase in frictions at the wall and interface and slows down the water flow. This, in turn, induces a higher gas velocity and hence an earlier formation of unstable wave growth at the hydraulic jump.

The CCFL data obtained from the data bank with 4 different L/D s are shown in Fig. 3. These 4 data sets are selected such that they represent various ranges of L/D from the different sources of experiments available. Since a larger L/D corresponds to a longer horizontal pipe length for a given pipe diameter, the lower L/D , the higher the flooding curve in Fig. 3.

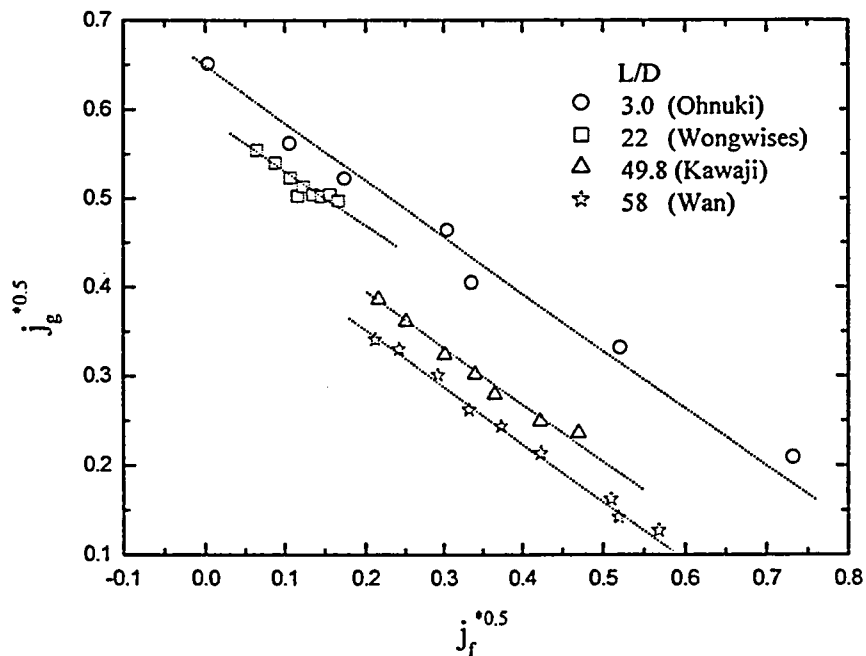


Fig. 3. Effect of Horizontal Pipe Length-to-Diameter Ratio on CCFL

2.2. Inclination Angle (θ) of Elbow Effect on CCFL

The variation of the inclination angle (θ) of elbow in the present data bank ranges from 35° to 90° . To compare the flooding points for different inclination angle of elbow, 3 data sets from Wongwises ($L/D = 22$) and 1 data set from Kang ($L/D = 25$) are selected and plotted in Fig. 4. The flooding points with different θ show the similar results indicating that the θ effect on them is not so clear as in the case of the L/D effect on CCFL.

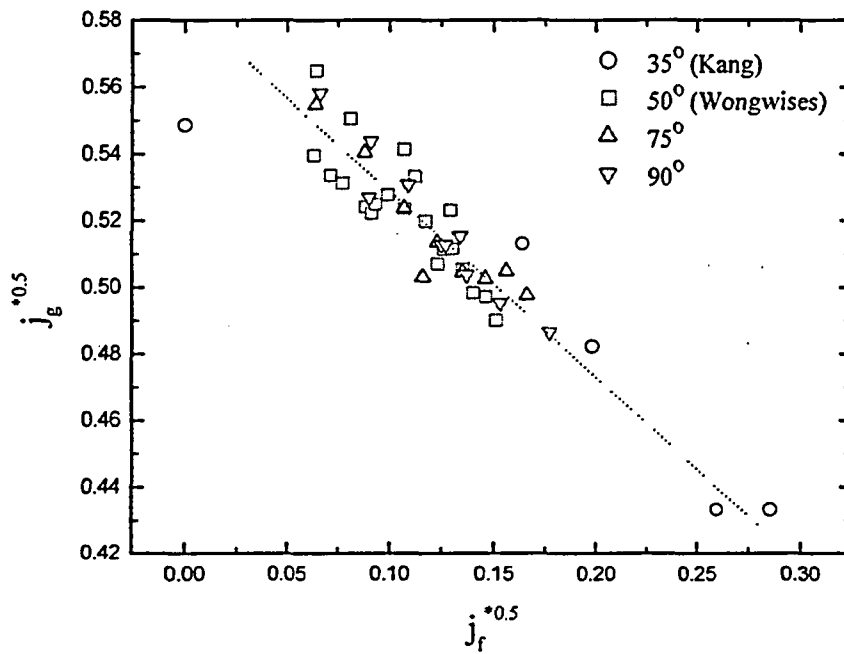


Fig. 4. Effect of Inclination Angle of Elbow on CCFL

2.3. Development of Empirical Flooding Correlation

Most of the existing data on CCFL are empirically correlated by the form of the Wallis correlation as:

$$j_g^{*0.5} + m j_f^{*0.5} = c. \quad (5)$$

Knowing that the deviation of the data points in Fig. 2 is mainly due to the L/D effect, the best fitting correlation is developed for the prediction of flooding points. The regression of the existing data points is conducted to find the constant, m , and the gas intercept, c . The following empirical correlation based on the present data bank is derived:

$$j_g^{*0.5} + 0.614 j_f^{*0.5} = 0.635 - 0.00254 \left(\frac{L}{D} \right). \quad (6)$$

The L/D effect on CCFL is also considered in Ohnuki's correlation and Kang's correlation as follows:

$$j_g^{*0.5} + 0.75 j_f^{*0.5} = \ln \left[\left(\frac{L}{D} \right) \left(\frac{1}{I} \right) \right]^{-0.066} + 0.88, \quad \text{for Ohnuki's correlation} \quad (7)$$

$$j_g^{*0.5} + 0.397 j_f^{*0.5} = 0.603 - 0.00234 \left(\frac{L}{D} \right), \quad \text{for Kang's correlation} \quad (8)$$

where I is the length of the riser (inclined section).

The predictions of the empirical correlations are compared with the experimental flooding data bank. Comparison of the present correlation with the database is displayed graphically in Fig. 5 and the percentage error is defined as:

$$\text{error}(\%) = \frac{1}{n} \times \sum \left| \frac{j_{gc}^{*0.5} - j_{fp}^{*0.5}}{j_{fp}^{*0.5}} \right| \times 100\%, \quad (9)$$

where

n = total number of flooding data points

$j_{gp}^{*0.5}$ = predicted flooding gas dimensionless superficial velocity

$j_{ge}^{*0.5}$ = experimental flooding gas dimensionless superficial velocity

The present empirical correlation agrees well with the database within the prediction error, 8.7%. Ohnuki's correlation predicts Ohnuki's data within 9.4% and Kang's correlation predicts Kang's data within 2.9%. However, the Ohnuki's correlation and the Kang's correlation have the prediction errors, 12.2% and 10.7% for the all database, respectively.

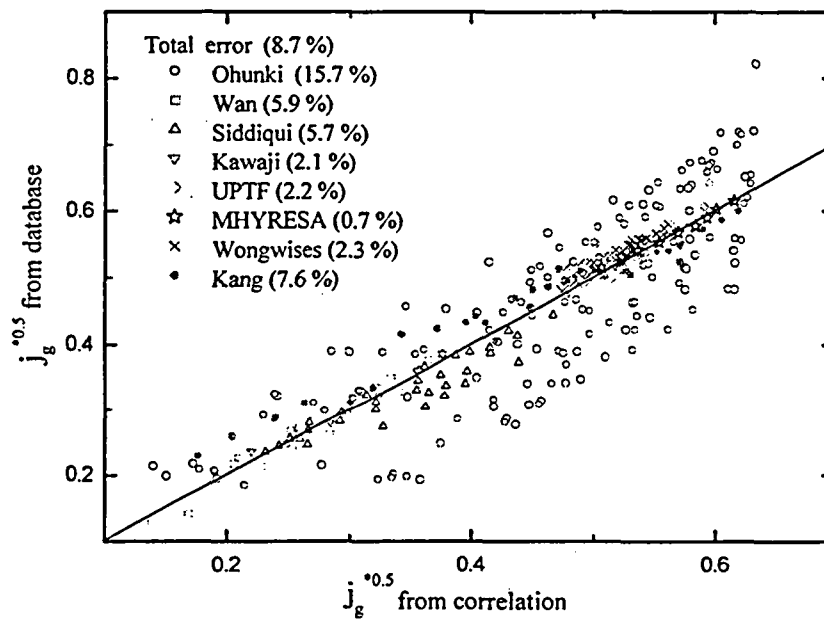


Fig. 5. Comparison between the Present Database and Empirical Correlation

NO and Choi (1995) developed a flooding correlation from their experimental studies of flooding in nearly horizontal pipes. It is interesting that NO and Choi's flooding data are well predicted by the present empirical correlation as shown in Fig. 6.

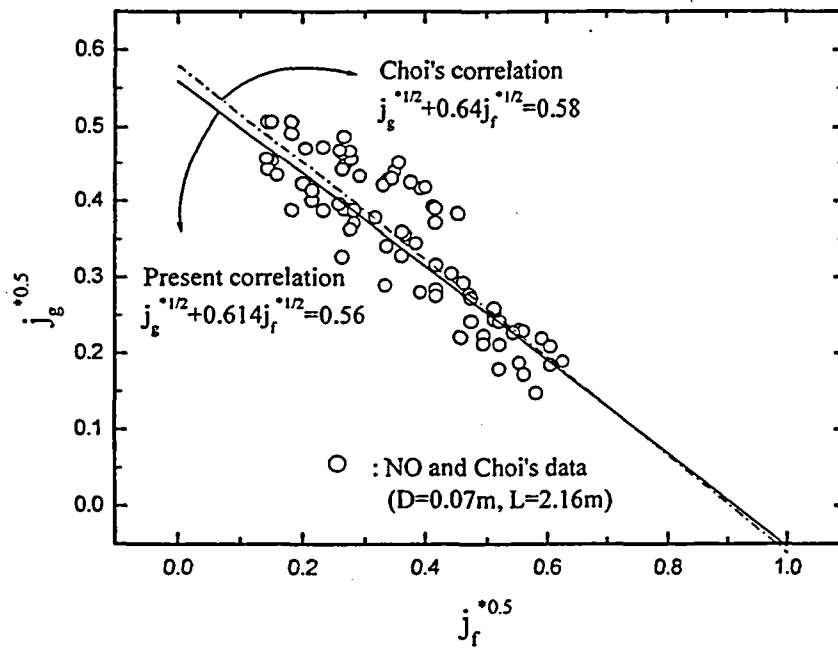


Fig. 6. Comparison between the Present Empirical Correlation and NO and Choi's Data

3. RELAP5 Model

3.1. Code Description

The assessment calculation for sample problems and CCFL experiments in the database are done using RELAP5/MOD3.2.2 γ computer code fixed for crossflow junction subscripts. Subscript errors were discovered by Won-Jai Lee (KAERI) in the *vexplt* subroutine for the crossflow junctions. These errors are known to affect the crossflow wall friction. Therefore, in a problem like CCFL, which has a cell with a crossflow junction, the patched code should be used. The correction in the *vexplt* subroutine was to change the *kf* and *lf* subscripts on *rhof* and *rhog* to *k* and *l*, respectively. The code is patched on SUNW SPARCstation 20 system operating under Solaris 2.6. The computer is a 32-bit workstation with 128MB of RAM memory and 167 MHz of clock speed.

In this study assessment of version 3.2.2 Gamma for CCFL in the horizontal-to-inclined pipes is done and the standard version is improved, as is the standard practice for developmental versions of RELAP5.

3.2. RELAP5 Nodalization

RELAP5 nodalization is developed for the simulation of the experimental results as shown in Fig. 7. The RELAP5 nodalization used in the present calculation is fixed to the same type as the CCFL test facility at KAIST (Kang's experiment).

Water is injected into the test section (Pipe-100) from the right plenum (Branch-340) and air from the left plenum (Pipe-230). Flow boundary conditions of water and air are modelled as time dependent junctions, TDV-315 and TDV-215, respectively. Water is drained into the left plenum (Pipe-230) and the time dependent junction, TDJ-250, controls the water inventory in the left plenum such that the

water flow rate to water outlet (TDV-260) is equal to one from the test section. Air flows out to the right plenum and flows up into the upper plenum (Pipe-350). And then air is vented to the time dependent volume, TDV-360, that is modelled as a pressure boundary.

The test section is modelled as a pipe component divided into horizontal volumes and inclined volumes. Flow area and the horizontal volume length of the test section are determined by D and L from the database. The inclination angle (θ) of the elbow is applied to the inclined volumes.

3.3. Simulation Procedure

The RELAP5 calculations follow the experimental procedures of allowing the liquid flow to settle down into a steady state before increasing the gas injection rate. Water flow is ramped up from zero to a given flow rate corresponding to the dimensionless superficial liquid velocity of the simulated database. While the water flow is maintained constant, the air flow is increased slowly until the onset of flooding is observed.

The onset of horizontal flooding is brought out, in RELAP5, by the rapid and very large increase of interface friction, which happens as the flow regime changes from stratified to slug flow. And the transition from stratified to slug flow induces the oscillatory behavior of void fraction, mass flow rate, pressure. Figure 8 shows the behavior of mass flow rates of liquid and gas during the simulation of the onset of CCFL.

At the moment the liquid flow rate in the horizontal test section has limitation and shows the fluctuation, the flooding gas flow rate is roughly determined. And after some trial and error calculations for the fixed water and air flow rates, we can obtain more correct flooding points.

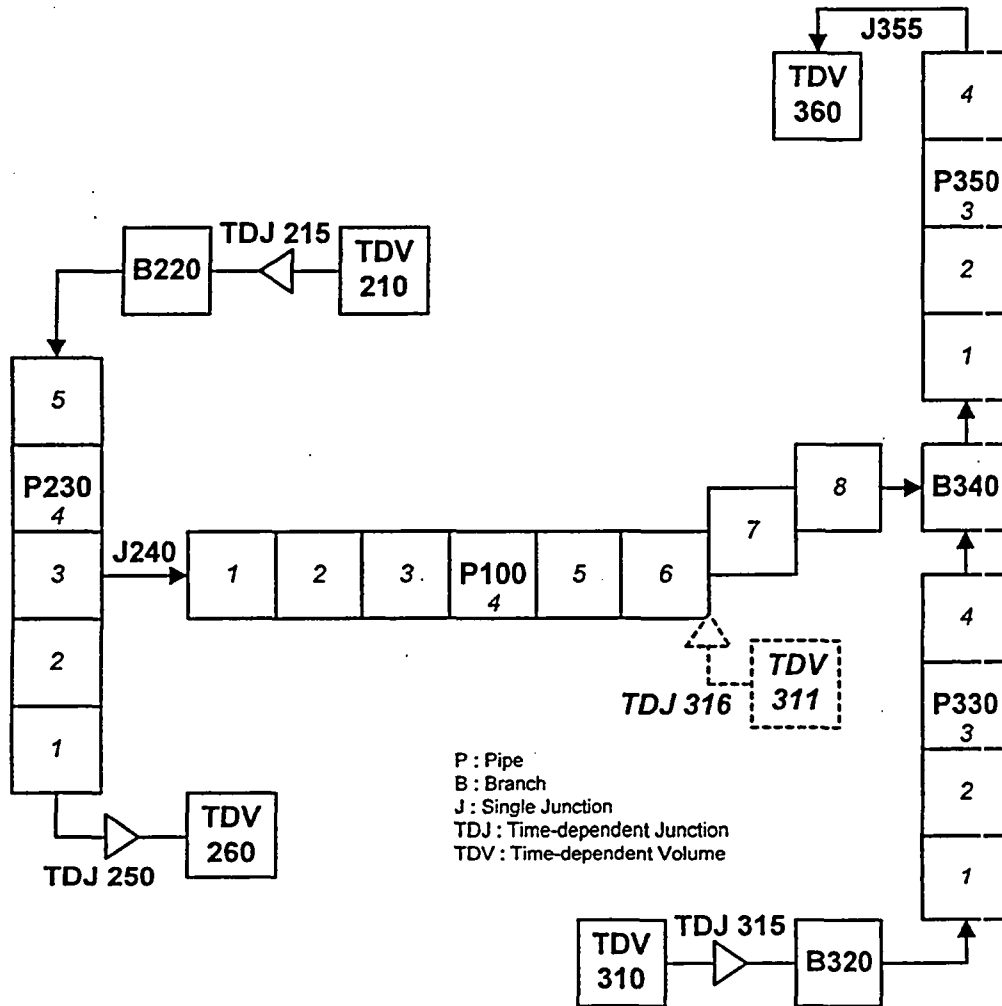


Fig. 7. RELAP5 Nodalization of CCFL Test in a Horizontal-to-Inclined Pipe

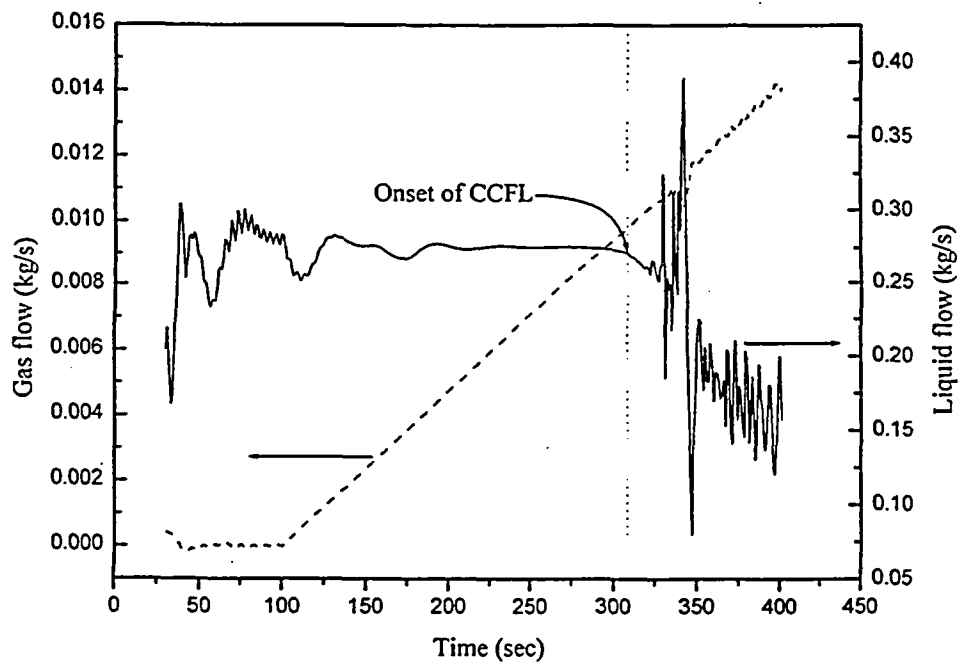


Fig. 8. Variation of Gas and Liquid Flow Rates at the Onset of CCFL

4. Code Calculations of the Database

4.1. Length-to-Diameter Ratio (L/D) Effect on RELAP5 Predictions

The experimental results with different L/Ds are simulated by RELAP5. For each dimensionless liquid superficial velocity from experimental data the critical gas superficial velocity is obtained by RELAP5. The range of L/D is from 3.0 to 58.0 as shown in Fig. 9. The relationship between L/Ds and critical gas flow rates required to initiate CCFL is also confirmed in RELAP5 calculations. Comparing the RELAP5 results with experimental data, we can see that RELAP5 predicts the flooding points closely but higher gas flow rates than those from real data where L/D is as low as that of the hot legs of typical PWRs.

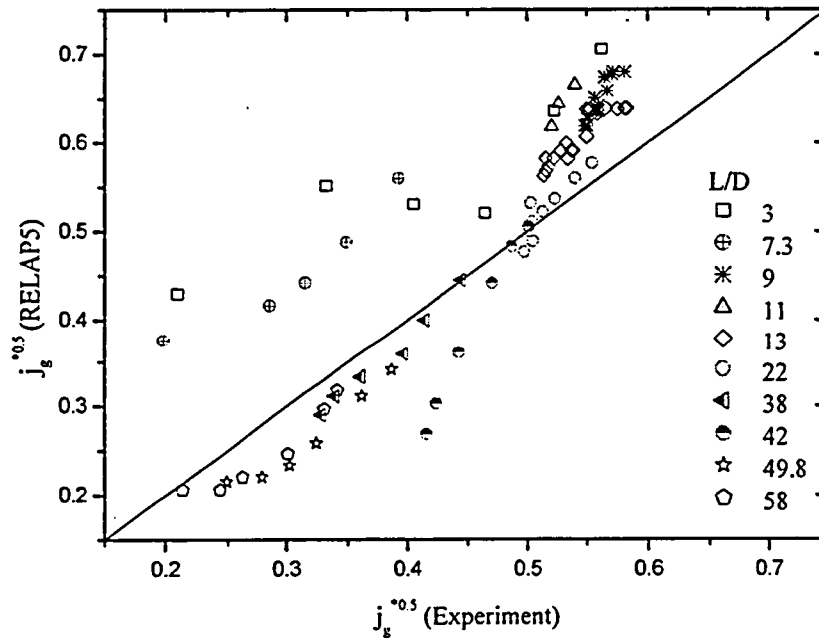


Fig. 9. Comparison of RELAP5 with Experimental Results with Various L/Ds

4.2. Inclination Angle (θ) of Elbow Effect on RELAP5 Predictions

RELAP5 calculations are compared with the flooding data points for different inclination angles. To avoid the L/D effects on CCFL, the experimental results with the same L/D (=25) are simulated by RELAP5. The calculation results and experimental data are plotted in Fig. 10. The percentage error between RELAP5 results and data points is within 2%. In RELAP5 calculations the flooding points are always the same for the different inclination angles, because the CCFL in the inclined region is less restrictive than that in the horizontal region.

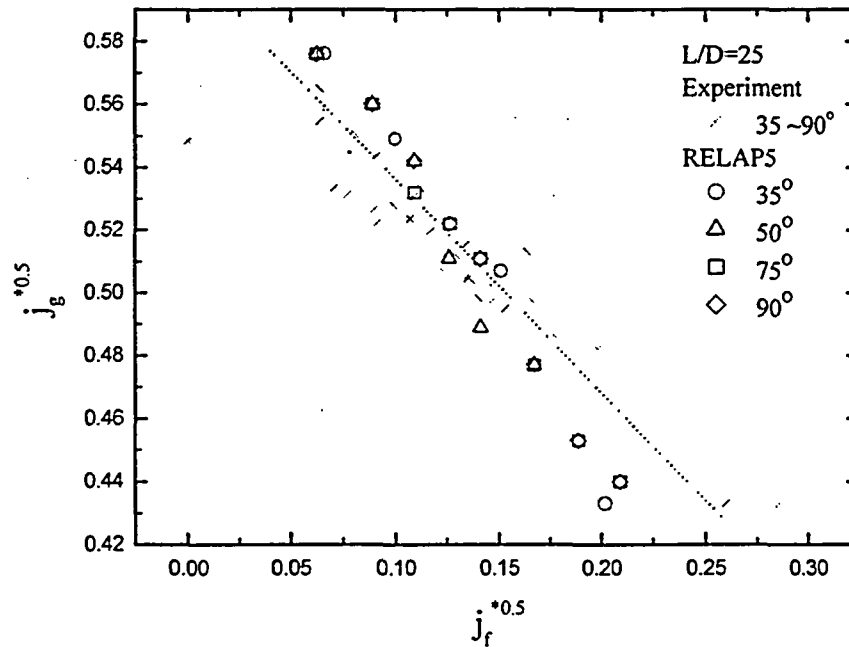


Fig. 10. Effect of Inclination Angle on RELAP5 Calculations

5. Application of Empirical Flooding Correlation to RELAP5

5.1. Modification of RELAP5/MOD3.2.2 γ

The original CCFL model in the standard version is used only for the volume cell whose inclination angle is higher than 45 degree (vertical volume). However, the restriction of the inclination angle on the application of CCFL model is removed. The flow chart of the CCFL subroutine in the standard version is shown in Fig. 11. In the CCFL subroutine of the modified version we comment on the if statement that checks if the volume is vertically oriented (see Appendix B).

The R-level input processing subroutines, such as RPIPE, RSNGJ and RBRNCH are modified to apply the present CCFL correlation to the CCFL model of the modified version, as shown in Fig. 12.

If one wishes to use the present CCFL correlation, he must specify 2.0 and L/D, for word 2 (form selector) and for word 3 (gas intercept) of CCFL data card (ccc1401~ccc1499, for pipe component), respectively. The input requirement of the new CCFL model is shown in Table 2. If $\beta \neq 2.0$, the CCFL model of the modified version is the same as that of the standard version.

It is known that the frictional drags and CCFL curve given by user mainly characterize the flooding process. If the CCFL by wall friction is more dominant than that by CCFL correlation, flooding occurs at lower gas velocity than predicted by the CCFL curve in standard RELAP5. Therefore, digit f of the volume control flag in the cell volumes is specified as 1 so that wall friction effects are not to be computed in the test section.

Table 2. Input Requirement for CCFL Data Card

	Word #1	Word #2	Word #3	Word #4
Original Input	Diameter	Form selection (β)	Gas intercept (c)	Slope (m)
Modified Input	Diameter	2.0	L/D	0.0 (or slope)

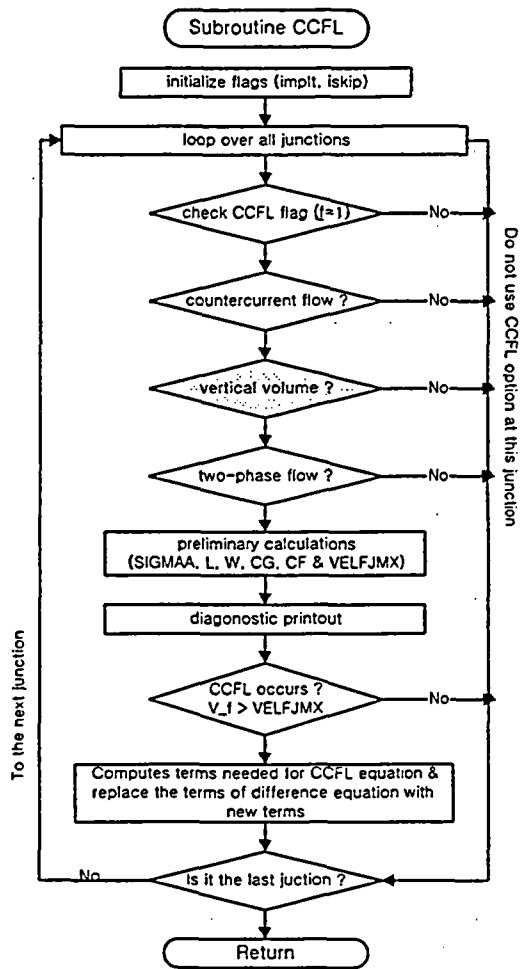


Fig. 11. Flow Chart of the Subroutine CCFL

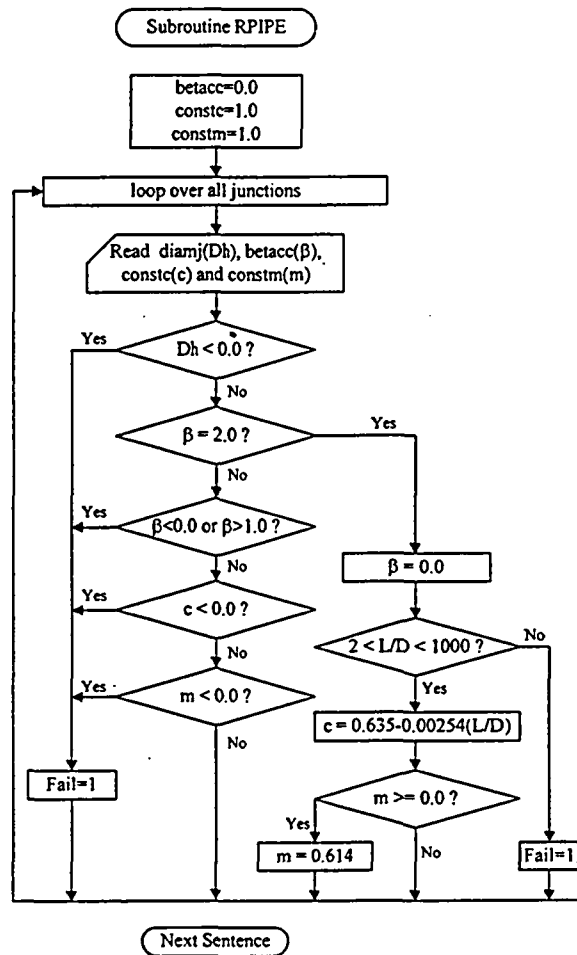


Fig. 12. Flow Chart of the Modified Subroutine RPIPE

5.2. Comparison of Code Calculation Results by Standard and Modified Versions.

The calculation results by the modified version are compared with those by the standard version.

It is shown that the present flooding correlation is successfully implemented to standard RELAP5 in Figs. 13 and 14 where the flooding limits of the empirical correlation are higher or lower than the predictions of standard RELAP5, respectively. For a given liquid flow rate, the gas flow rate is increased to reach the flooding curve, and then the calculation results of the modified RELAP5 lie well on the line given by the empirical correlation.

In Fig. 13 L/D is such a small value that the standard RELAP5 predicts the higher gas flow than the experimental data. In this case, the flooding criterion is satisfied before the interfacial and the wall drags initiate CCFL. When L/D is high as shown in Fig. 14, the onset of flooding occurs before the flooding limit by the correlation is applied in the RELAP5 calculation. If we set the f digit of the volume control flag to 1 in the horizontal test section RELAP5 predictions by the modified version lie well on the flooding line as shown in Fig. 14.

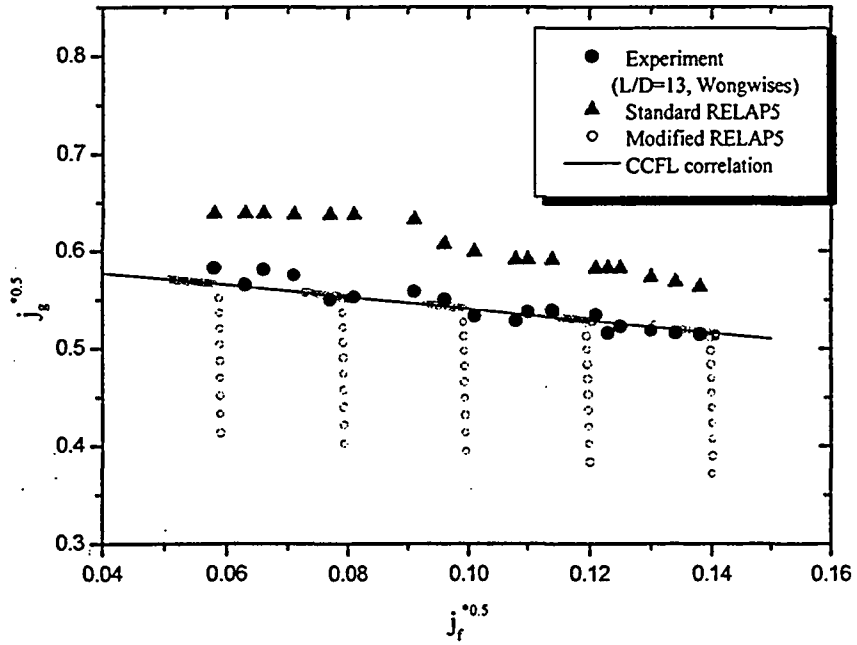


Fig. 13. Comparison of Experimental Data with Small L/D With Predictions by Standard & Modified RELAP5

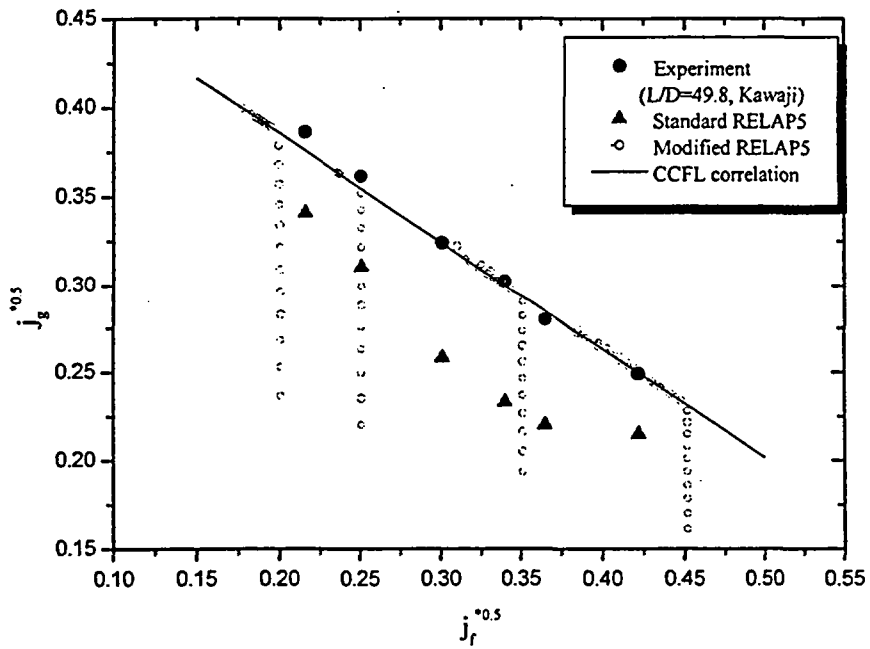


Fig. 14. Comparison of Experimental Data with Large L/D With Predictions by Standard & Modified RELAP5

6. Conclusions

A total of 356 experimental data for the onset of flooding are compiled for the data bank and used for the assessment of RELAP5/MOD3.2.2y predictions of Counter-Current Flow Limitation (CCFL) in horizontal-to-inclined pipes simulating a PWR hot leg. From the present study the following conclusions can be made.

- 1) The dimensionless Wallis-type gas velocities and liquid velocities are identified with the geometrical conditions such as horizontal pipe diameter (D), length (L) and the inclination angle (θ) of the bend. The experimental data show that the flooding curve becomes higher with the lower L/D while their θ effect on CCFL is not found.
- 2) The RELAP5 calculations are compared with the experimental data where L/D is varied within the range of database. The L/D effect on CCFL is also confirmed in RELAP5 results, but higher gas flow rate is required to initiate the flooding compared with the experimental data if the L/D is as low as that of the hot legs of typical PWRs.
- 3) The best fitting correlation is developed for the prediction of flooding points, which shows the L/D effect. The present correlation agrees well with the database within the prediction error, 8.7%. The result of empirical correlation based on the present data bank is as follows:

$$j_g^{*0.5} + 0.614 j_f^{*0.5} = 0.635 - 0.00254 \left(\frac{L}{D} \right).$$

- 4) The present flooding correlation is implemented into the standard RELAP5 and validated against the data bank. It is shown that the present flooding correlation is successfully implemented to the standard RELAP5 for the both cases where, flooding limit of the empirical correlation is higher or lower than the predictions of standard RELAP5.

References

1. Richard A. Riemke, "Countercurrent Flow Limitation Model for RELAP5/MOD3", Nuclear Technology 93, pp. 166-173, 1991.
2. Sun Heo, Hee Cheon NO, "Improvement of The CCFL Models of the RELAP5/MOD3.2.2B Code in a Horizontal Pipe", Proc. 8th International Conference on Nuclear Engineering, Baltimore, USA, 2000.
3. A. Ohnuki, "Experimental Study of Counter-Current Two-Phase Flow in Horizontal Tube Connected to Inclined Riser", J. of Nuclear Science and Technology 23 (3), pp. 219-232, 1986.
4. P.T. Wan, V.S. Krishnan, "Air-Water Flooding in 90° Elbow with a Slightly Inclined Lower Leg", Proc. CN 7th Annual Conf., Toronto, 1986.
5. H. Siddiqui, S. Banerjee, K.H. Ardron, "Flooding in a Elbow Between a Vertical and a Horizontal or Near-Horizontal Pipe", Int. J. Multiphase Flow 12 (4), pp. 531-541, 1986.
6. M. Kawaji, L.A. Thomson, V.S. Krishnan, "Countercurrent Flooding in Vertical-to-Inclined Pipes", Experimental Heat Transfer 4, pp. 95-110, 1991.
7. S. Wongwises, "Two-Phase Countercurrent Flow in a Model of a Pressurized Water Reactor Hot Leg", Nuclear Engineering and Design 166, pp. 121-133, 1996.
8. S.K. Kang, Hee Cheon NO, "Air-Water Countercurrent Flow Limitation in a Horizontal Pipe Connected to an Inclined Riser", J. Korean Nuclear Society 31 (6), pp. 548-560, 1999.
9. K.Y. Choi, Hee Cheon NO, "Experimental Studies of Flooding in Nearly Horizontal Pipes", Int. J. Multiphase Flow 21 (3), pp. 419-436, 1995.

Appendix A. Sample Input Deck for CCFL Test

CCFL in horizontal pipe

* CCFL test input for the Siddiqui's CCFL experiment
 * Test section : D= 47 mm, L= 1820 + 1000 mm(?)
 * Simulation by Hyoung Tae Kim

100 new transnt
 101 run
 102 si
 105 10. 20.
 110 air
 120 100010000 0.0 h2o t-sec

* TIME STEP CONTROL
 * T_end T_min T_max ssdt minor major restart
 201 700. 1.e-7 0.01 00003 100 10000 10000

501 time 0 ge null 0 0.0 1 -1.0
 * air injection
 511 time 0 ge null 0 0.0 1 -1.0
 * water injection
 512 time 0 ge null 0 0.0 1 -1.0

311 cntrlvar 421 *Wf
 312 cntrlvar 431 *Wg
 316 cntrlvar 428 *jf*1/2
 317 cntrlvar 438 *jg*1/2

20541000 gdrho sum 0.4606 0.0 1
 * ----->9.8x0.047
 20541001 0.0 1.0 rhofj 100080000
 20541002 -1.0 rhogj 100080000

20541100 gdrho sum 1.0 1.0 1
 20541101 1.0e-4 1.0 cntrlvar 410

20542000 jf mult 1.0 0.0 1
 20542001 voidfj 100080000
 20542002 velfj 100080000

20542100 Wf mult -1.735e-3 0.0 1
 * -----> area
 20542101 rhofj 100080000
 20542102 cntrlvar 420

20542200 rf_gdr div 1.0 0.0 1
 20542201 cntrlvar 411
 20542202 rhofj 100080000

20542400 rf_gdr2 powerr 1.0 0.0 1
 20542401 cntrlvar 422 0.5

20542600 jf_s mult 1.0 0.0 1
 20542601 cntrlvar 420
 20542602 cntrlvar 424
 20542603 cntrlvar 420
 20542604 cntrlvar 424

20542800 jf_s2 powerr 1.0 0.0 1
 20542801 cntrlvar 426 0.25

*
 *
 20543000 jg mult 1.0 0.0 1
 20543001 voidgj 100080000
 20543002 velgj 100080000

*
 *
 20543100 Wg mult 1.735e-3 0.0 1
 * -----> area
 20543101 rhogj 100080000
 20543102 cntrlvar 430

*
 *
 20543200 rg_gdr div 1.0 0.0 1
 20543201 cntrlvar 411
 20543202 rhogj 100080000

*
 *
 20543400 rg_gdr2 powerr 1.0 0.0 1
 20543401 cntrlvar 432 0.5

*
 *
 20543600 jg_s mult 1.0 0.0 1
 20543601 cntrlvar 430
 20543602 cntrlvar 434
 20543603 cntrlvar 430
 20543604 cntrlvar 434

*
 *
 20543800 jg_s2 powerr 1.0 0.0 1
 20543801 cntrlvar 436 0.25

hydrodynamic model input for test section

Test Section

* component 100: test section

1000000 test-sec pipe
 1000001 15
 *
 * 01:area, 03:length, 04:volume
 1000101 1.735e-3 15
 1000301 0.182 10
 1000302 0.2 15
 1000401 0.0 15

* vertical angle
 1000601 0.0 10
 1000602 90.0 15

* roughness hyd. dia. / energy loss coeff.
 1000801 0.0002 0.047 15
 1000901 0.0 0.0 14

* tlpvbf / cfvcahs
 1001001 0000000 15
 1001101 0100000 7
 1001102 0100000 8
 1001103 0100000 14

* volume initial condition
 1001201 004 1.03e5 293.15 0.0 0.0 0.0 15

```

* junction initial condition
1001300 1
1001301 0.0 0.0 0.0 14
*
* ccf1 data card(dia, beta, c, m, no.)
*1001401 0.08 0.0 2.0 1.0 3
*1001402 0.08 2.0 25.0 0.0 4
*1001403 0.08 0.0 2.0 1.0 7
*
*-----
* Left part - air injection & water venting
*-----
* component 210 : TDV for the air injection
*
2100000 air_in tmdpvol
2100101 10.0 0.0 0.01 0.0 0.0 0.0
2100102 0.00001 0.0 00
*
2100200 004
2100201 0.0 1.03e5 293.15 0.0
*
* component 215: TDJ (from 210 to 220)
*
2150000 a_jun tmdpjun
*
2150101 210010000 220000000 1.735e-3
2150200 1 511
2150201 -1.0 0.00 0.00 0.00
2150202 0.0 0.00 0.00 0.00
2150203 2000.0 0.00 0.00 0.00
*
* component 220: air inlet pipe
*
2200000 airin branch
2200001 1 1
*
area length volume angle(az/inc) elev
2200101 1.735e-3 0.5 0.0 0.0 0.0 0.0
*
roughness dia. tlpvbf
2200102 0.0002 0.0 010
2200200 004 1.03e5 293.15 0.0
*
from to area
2201101 220010000 230050003 1.735e-3 0.0 0.0 00
*
2201201 0.0 0.0 0.0
*
* component 230 : water venting tank
*
2300000 w-vent pipe
2300001 5
*
01:area, 03:length
2300101 0.11 5
2300301 0.047 2
2300302 0.047 3
2300303 0.047 5
*
vertical angle
2300601 90.0 5
*
roughness hyd. dia. / energy loss coeff.(FW/R)
2300801 0.0 0.0 5
2300901 0.0 0.0 4
*
tlpvbf / cfvcahs

```

```

2301001 0000000 5
2301101 0000000 4
*
2301201 003 1.03e5 293.15 0.0 0.0 0.0 1
2301202 004 1.03e5 293.15 0.0 0.0 0.0 3
2301203 004 1.03e5 293.15 0.0 0.0 0.0 5
*
junction initial condition
2301300 1
2301301 0.0 0.0 0.0 4
*
* component 240: single junction (from 230-03 to 100)
*
2400000 air-inj sngljun
*
from to area
2400101 230030003 100000000 1.735e-3 0.0 1.0 00
2400201 1 0.0 0.0 0.0
*
* component 250: TDJ(water out)
*
2500000 wt_out tmdpjun
*
2500101 230000000 260000000 1.8e-2
2500200 1 501 cntrlvar 421
2500201 -1.0 0.0 0.00 0.00
2500202 0.0 0.0 0.00 0.00
2500203 1.0 1.0 0.00 0.00
2500204 100.0 100.0 0.00 0.00
*
* component 260 : TDV for the water outlet
*
2600000 wt_out tmdpvol
2600101 10.0 0.0 0.01 0.0 0.0 0.0
2600102 0.00001 0.0 00
*
2600200 003
2600201 0.0 1.03e5 293.15
*
*-----
* Right part - water injection & air venting
*-----
* component 310 : TDV for the water injection
*
3100000 wt_in tmdpvol
3100101 10.0 0.0 0.01 0.0 0.0 0.0
3100102 0.00001 0.0 00
*
3100200 003
3100201 0.0 1.03e5 293.15
*
* component 315: TDJ (from 310 to 320)
*
3150000 w_jun tmdpjun
*
3150101 310010000 320000000 1.735e-3
3150200 1 512
3150201 -1.0 0.0 0.00 0.00
3150202 0.0 0.0 0.00 0.00
3150203 2000.0 0.0 0.00 0.00
*
*-----> for the liquid film correction -----

```



```

*
* component 311 : TDV for the water injection
*
3110000 wt_in tmdpvol
3110101 10.0 0.0 0.01 0.0 0.0 0.0
3110102 0.00001 0.0 00
*
3110200 003
3110201 0.0 1.03e5 293.15
*
* component 316: TDJ (from 311 to 316)
*
3160000 w_jun tmdpjun
*
3160101 311010000 100100002 1.735e-4
3160200 1 512
3160201 -1.0 0.0 0.00 0.00
3160202 0.0 0.0 0.00 0.00
3160203 2000.0 0.0 0.00 0.00
*
*-----
*
* component 320: water injection line
*
3200000 w_inj branch
3200001 1 1
*
* area length volume angle(az/inc) elev
3200101 1.735e-3 0.5 0.0 0.0 0.0 0.0
*
* roughness dia. tlpvbf
3200102 0.0002 0.0 0000010
3200200 003 1.03e5 293.15
*
* from to area
3201101 320010000 330000000 1.735e-3 0.0 0.0 00
*
3201201 0.0 0.0 0.0
*
* component 330: water tank
*
3300000 wtnk pipe
3300001 4
*
* 01:area, 03:length, 04:volume
3300101 0.11 4
3300301 0.1 4
3300401 0.0 4
*
* vertical angle
3300601 90.0 4
*
* roughness hyd. dia. / energy loss coeff.
3300801 0.0002 0.0 4
3300901 0.0 0.0 3
*
* tlpvbf / efvcahs
3301001 0000000 4
3301101 0000000 3
*
* volume initial condition
3301201 003 1.03e5 293.15 0.0 0.0 0.0 4
*
* junction initial condition
3301300 1

```

```

3301301 0.0 0.0 0.0 3
*
* component 340: right-section
*
3400000 right branch
3400001 3 1
*
* area length volume angle(az/inc) elev
3400101 0.11 0.047 0.0 0.0 90.0 0.047
*
* roughness dia. tlpvbf
3400102 0.0002 0.0 0000000
3400200 004 1.03e5 293.15 0.0
*
* from to area
3401101 100010000 340010003 1.735e-3 0.0 0.0 00
3402101 330010000 340000000 0.11 0.0 0.0 00
3403101 340010000 350000000 0.11 0.0 0.0 00
*
3401201 0.0 0.0 0.0
3402201 0.0 0.0 0.0
3403201 0.0 0.0 0.0
*
* component 350: air venting pipe
*
3500000 air-out pipe
3500001 4
*
* 01:area, 03:length, 04:volume
3500101 0.11 4
3500301 0.4 4
3500401 0.0 4
*
* vertical angle
3500601 90.0 4
*
* roughness hyd. dia. / energy loss coeff.
3500801 0.0002 0.0 4
3500901 0.0 0.0 3
*
* tlpvbf / efvcahs
3501001 0000000 4
3501101 0000000 3
*
* volume initial condition
3501201 004 1.03e5 293.15 0.0 0.0 0.0 4
*
* junction initial condition
3501300 1
3501301 0.0 0.0 0.0 3
*
* component 355: single junction (from 350 to 360)
*
3550000 air-outj sngljun
*
* from to area
3550101 350010000 360000000 0.002 10.0 0.0 00
3550201 1 0.0 0.0 0.0
*
* component 360 : TDV for the air venting
*
3600000 air-tdv tmdpvol
3600101 10.0 0.0 0.01 0.0 90.0 0.001

```

```

3600102  0.00001  0.0  00
*
3600200  004
3600201  0.0  1.03e5  293.15  0.0
*
*
=====
*  MODIFICATION - Water & Air injection rate
=====
*  TIME STEP CONTROL
*  T_end T_min T_max  ssdt  minor  major  estart
201  500.  1.e-8  0.05  00003  10  6000  6000
*
*
*  AIR
2150203  200.0  0.00  0.008  0.00
2150204  300.0  0.00  0.008  0.00
*
*  WATER
3150201  -1.0  0.00  0.00  0.00
3150202  0.0  0.00  0.00  0.00
3150203  10.0  0.0158  0.00  0.00
3150204  500.0  0.0158  0.00  0.00
*
3160202  0.0  0.0158e-2  0.00  0.00
3160203  10.0  0.0158e-2  0.00  0.00
*
*
*  . End of file
*
*  water(kg/s)  air(kg/s)  jf  jg
*  0.0158  0.008  0.117  0.445
*  0.031  0.0065  0.163  0.40
*  0.046  0.0052  0.199  0.359
*  0.061  0.0045  0.229  0.333
*  0.078  0.0039  0.259  0.311
*  0.093  0.0034  0.283  0.29

```

Appendix B. Modified parts in the RELAP5 Subroutines

B.1 Subroutine ccfl.f

#79 line

c Perform preliminary calculations.

cblh-----

cblh if (iand(jcex(i),4) .eq. 0) go to 1990

 if (.not.isnpccflg2(2,i)) go to 1990

cblh-----

cblh-----

cblh jcex(i) = iand(jcex(i),not(2))

cblh-----

cblh if (iand(jc(i),2).ne.0 .or. velfj(i)*velgj(i).ge.0.0)

cblh * go to 1990

 iscclflg1(2,i) = .false.

cblh-----

 if(istdpjunflg1(2,i) .or. velfj(i)*velgj(i)

 & .ge. 0.0d0) goto 1990

cblh-----

 k = ij1nx(2,i)

cblh-----

cblh kx = k + iand(ishft(jcex(i),-13),3)

c **kx = k + fromface1214(2,i)/2**

cblh-----

 l = ij2nx(2,i)

cblh-----

cblh lx = l + iand(ishft(jcex(i),-10),3)

c **lx = l + toface911(2,i)/2**

cblh-----

cblh nmapk = iand(imap(kx),63)

cblh-----

c **nmapk = ismapinfo05(2,kx)**

```
cblh-----  
cblh-----  
cblh      nmapl = iand(imap(lx),63)  
c      nmapl = ismapinfo05(2,lx)  
cblh-----  
c      if (nmapk.eq.2 .or. nmapl.eq.2) go to 1990  
c      delzk = hydzc(kx)  
cblh-----  
cblh      if (iand(jc(i),4) .ne. 0) delzk = -delzk  
c      if(isrevfrmvolconflg2(2,i)) delzk = -delzk  
cblh-----  
c      delzl = hydzc(lx)  
cblh-----  
cblh      if (iand(jc(i),8) .ne. 0) delzl = -delzl  
c      if(isrevtovolconflg3(2,i)) delzl = -delzl  
cblh-----  
c      if (delzk*delzl .le. 0.0d0) go to 1990
```

B.2 Subroutine rpipe.f

#1849 line

```
do 609 k = ij,ije,ijskp
    if (diamj(k) .lt. 0.0d0) then
        diamj(k) = 0.0d0
        tfail = .true.
    endif
c     if (betacc(k).lt.0.0d0.or. betacc(k).gt.1.0d0) then
c         betacc(k) = 0.0d0
c         tfail = .true.
c     endif
c     if (constc(k) .le. 0.0d0) then
c         constc(k) = 0.0d0
c         tfail = .true.
c     endif
c     if (constm(k) .le. 0.0d0) then
c         constm(k) = 0.0d0
c         tfail = .true.
c     endif
    if (betacc(k).gt.1.99 .and. betacc(k).lt.2.01) then
        betacc(k) = 0.0
        if (constc(k) .lt. 2.0 .or. constc(k) .gt. 1000.0) then
            constc(k) = 0.0
            tfail = .true.
        else
c         New CCFL correlation
            constc(k) = 0.635 - 0.00254 * constc(k)
        endif
    endif
```

```
if (constm(k) .ge. 0.0) then
  constm(k)=0.614
else
  tfail = .true.
endif
else
  if (betacc(k).lt.0.0 .or. betacc(k).gt.1.0) then
    betacc(k) = 0.0
    tfail = .true.
  endif
  if (constc(k) .le. 0.0) then
    constc(k) = 0.0
    tfail = .true.
  endif
  if (constm(k) .le. 0.0) then
    constm(k) = 0.0
    tfail = .true.
  endif
endif
endif
```

c

609 continue

Appendix C. Flooding Database

No.	Author	P [MPa]	D [m]	L [m]	L/D [m]	θ	l [m]	$j_f^{0.5}$	$j_g^{0.5}$
1	Ohnuki	0.1	0.026	0.01	0.385	40	0.1	0.002	0.722
2	Ohnuki	0.1	0.026	0.01	0.385	40	0.1	0.060	0.673
3	Ohnuki	0.1	0.026	0.01	0.385	40	0.1	0.087	0.639
4	Ohnuki	0.1	0.026	0.01	0.385	40	0.1	0.182	0.590
5	Ohnuki	0.1	0.026	0.01	0.385	40	0.1	0.229	0.553
6	Ohnuki	0.1	0.026	0.01	0.385	40	0.1	0.304	0.494
7	Ohnuki	0.1	0.026	0.01	0.385	40	0.1	0.373	0.448
8	Ohnuki	0.1	0.026	0.01	0.385	40	0.1	0.446	0.393
9	Ohnuki	0.1	0.026	0.01	0.385	40	0.1	0.540	0.320
10	Ohnuki	0.1	0.026	0.01	0.385	40	0.1	0.722	0.205
11	Ohnuki	0.1	0.026	0.04	1.538	40	0.1	0.002	0.641
12	Ohnuki	0.1	0.026	0.04	1.538	40	0.1	0.106	0.554
13	Ohnuki	0.1	0.026	0.04	1.538	40	0.1	0.146	0.519
14	Ohnuki	0.1	0.026	0.04	1.538	40	0.1	0.237	0.468
15	Ohnuki	0.1	0.026	0.04	1.538	40	0.1	0.352	0.423
16	Ohnuki	0.1	0.026	0.04	1.538	40	0.1	0.446	0.363
17	Ohnuki	0.1	0.026	0.04	1.538	40	0.1	0.573	0.299
18	Ohnuki	0.1	0.026	0.04	1.538	40	0.1	0.614	0.263
19	Ohnuki	0.1	0.026	0.04	1.538	40	0.1	0.679	0.185
20	Ohnuki	0.1	0.026	0.13	5.000	40	0.1	0.001	0.557
21	Ohnuki	0.1	0.026	0.13	5.000	40	0.1	0.077	0.516
22	Ohnuki	0.1	0.026	0.13	5.000	40	0.1	0.145	0.463
23	Ohnuki	0.1	0.026	0.13	5.000	40	0.1	0.247	0.391
24	Ohnuki	0.1	0.026	0.13	5.000	40	0.1	0.355	0.351
25	Ohnuki	0.1	0.026	0.13	5.000	40	0.1	0.562	0.215
26	Ohnuki	0.1	0.026	0.24	9.231	40	0.1	0.001	0.483
27	Ohnuki	0.1	0.026	0.24	9.231	40	0.1	0.125	0.464
28	Ohnuki	0.1	0.026	0.24	9.231	40	0.1	0.159	0.433
29	Ohnuki	0.1	0.026	0.24	9.231	40	0.1	0.187	0.416
30	Ohnuki	0.1	0.026	0.24	9.231	40	0.1	0.219	0.371
31	Ohnuki	0.1	0.026	0.24	9.231	40	0.1	0.271	0.343
32	Ohnuki	0.1	0.026	0.24	9.231	40	0.1	0.315	0.306
33	Ohnuki	0.1	0.026	0.24	9.231	40	0.1	0.363	0.285
34	Ohnuki	0.1	0.026	0.24	9.231	40	0.1	0.386	0.249
35	Ohnuki	0.1	0.026	0.24	9.231	40	0.1	0.450	0.202
36	Ohnuki	0.1	0.026	0.02	0.769	40	0.19	0.002	0.721
37	Ohnuki	0.1	0.026	0.02	0.769	40	0.19	0.062	0.669
38	Ohnuki	0.1	0.026	0.02	0.769	40	0.19	0.089	0.635
39	Ohnuki	0.1	0.026	0.02	0.769	40	0.19	0.127	0.607
40	Ohnuki	0.1	0.026	0.02	0.769	40	0.19	0.214	0.551

No.	Author	P [MPa]	D [m]	L [m]	L/D [m]	θ	l [m]	$j_f^{*0.5}$	$j_R^{*0.5}$
41	Ohnuki	0.1	0.026	0.02	0.769	40	0.19	0.301	0.512
42	Ohnuki	0.1	0.026	0.02	0.769	40	0.19	0.414	0.454
43	Ohnuki	0.1	0.026	0.02	0.769	40	0.19	0.499	0.389
44	Ohnuki	0.1	0.026	0.02	0.769	40	0.19	0.639	0.323
45	Ohnuki	0.1	0.026	0.02	0.769	40	0.19	0.785	0.199
46	Ohnuki	0.1	0.026	0.05	1.923	40	0.19	0.000	0.654
47	Ohnuki	0.1	0.026	0.05	1.923	40	0.19	0.083	0.601
48	Ohnuki	0.1	0.026	0.05	1.923	40	0.19	0.141	0.538
49	Ohnuki	0.1	0.026	0.05	1.923	40	0.19	0.198	0.504
50	Ohnuki	0.1	0.026	0.05	1.923	40	0.19	0.295	0.444
51	Ohnuki	0.1	0.026	0.05	1.923	40	0.19	0.451	0.386
52	Ohnuki	0.1	0.026	0.05	1.923	40	0.19	0.562	0.390
53	Ohnuki	0.1	0.026	0.05	1.923	40	0.19	0.586	0.312
54	Ohnuki	0.1	0.026	0.05	1.923	40	0.19	0.713	0.195
55	Ohnuki	0.1	0.026	0.08	3.077	40	0.19	0.000	0.621
56	Ohnuki	0.1	0.026	0.08	3.077	40	0.19	0.078	0.559
57	Ohnuki	0.1	0.026	0.08	3.077	40	0.19	0.133	0.522
58	Ohnuki	0.1	0.026	0.08	3.077	40	0.19	0.246	0.464
59	Ohnuki	0.1	0.026	0.08	3.077	40	0.19	0.309	0.402
60	Ohnuki	0.1	0.026	0.08	3.077	40	0.19	0.518	0.330
61	Ohnuki	0.1	0.026	0.08	3.077	40	0.19	0.740	0.217
62	Ohnuki	0.1	0.026	0.19	7.308	40	0.05	0.000	0.483
63	Ohnuki	0.1	0.026	0.19	7.308	40	0.05	0.056	0.453
64	Ohnuki	0.1	0.026	0.19	7.308	40	0.05	0.089	0.423
65	Ohnuki	0.1	0.026	0.19	7.308	40	0.05	0.136	0.393
66	Ohnuki	0.1	0.026	0.19	7.308	40	0.05	0.207	0.349
67	Ohnuki	0.1	0.026	0.19	7.308	40	0.05	0.261	0.315
68	Ohnuki	0.1	0.026	0.19	7.308	40	0.05	0.306	0.286
69	Ohnuki	0.1	0.026	0.19	7.308	40	0.05	0.440	0.198
70	Ohnuki	0.1	0.026	0.01	0.385	40	0.1	0.000	0.822
71	Ohnuki	0.1	0.026	0.01	0.385	40	0.1	0.048	0.718
72	Ohnuki	0.1	0.026	0.01	0.385	40	0.1	0.088	0.673
73	Ohnuki	0.1	0.026	0.01	0.385	40	0.1	0.131	0.643
74	Ohnuki	0.1	0.026	0.01	0.385	40	0.1	0.191	0.617
75	Ohnuki	0.1	0.026	0.01	0.385	40	0.1	0.281	0.568
76	Ohnuki	0.1	0.026	0.01	0.385	40	0.1	0.358	0.524
77	Ohnuki	0.1	0.026	0.01	0.385	40	0.1	0.470	0.457
78	Ohnuki	0.1	0.026	0.01	0.385	40	0.1	0.644	0.326
79	Ohnuki	0.1	0.026	0.01	0.385	40	0.1	0.723	0.207
80	Ohnuki	0.1	0.026	0.01	0.385	40	0.1	0.545	0.390

No.	Author	P [MPa]	D [m]	L [m]	L/D [m]	θ	l [m]	$J_f^{*0.5}$	$J_g^{*0.5}$
81	Ohnuki	0.1	0.026	0.19	7.308	40	0.05	0.000	0.559
82	Ohnuki	0.1	0.026	0.19	7.308	40	0.05	0.065	0.514
83	Ohnuki	0.1	0.026	0.19	7.308	40	0.05	0.195	0.451
84	Ohnuki	0.1	0.026	0.19	7.308	40	0.05	0.231	0.388
85	Ohnuki	0.1	0.026	0.19	7.308	40	0.05	0.323	0.318
86	Ohnuki	0.1	0.026	0.19	7.308	40	0.05	0.460	0.196
87	Ohnuki	0.1	0.026	0.08	3.077	40	0.19	0.005	0.611
88	Ohnuki	0.1	0.026	0.08	3.077	40	0.19	0.051	0.561
89	Ohnuki	0.1	0.026	0.08	3.077	40	0.19	0.071	0.534
90	Ohnuki	0.1	0.026	0.08	3.077	40	0.19	0.128	0.501
91	Ohnuki	0.1	0.026	0.08	3.077	40	0.19	0.222	0.453
92	Ohnuki	0.1	0.026	0.08	3.077	40	0.19	0.284	0.394
93	Ohnuki	0.1	0.026	0.08	3.077	40	0.19	0.457	0.322
94	Ohnuki	0.1	0.026	0.08	3.077	40	0.19	0.648	0.292
95	Ohnuki	0.1	0.026	0.08	3.077	40	0.19	0.793	0.214
96	Ohnuki	0.1	0.051	0.3	5.882	45	0.6	0.001	0.720
97	Ohnuki	0.1	0.051	0.3	5.882	45	0.6	0.043	0.658
98	Ohnuki	0.1	0.051	0.3	5.882	45	0.6	0.125	0.591
99	Ohnuki	0.1	0.051	0.3	5.882	45	0.6	0.211	0.508
100	Ohnuki	0.1	0.051	0.3	5.882	45	0.6	0.050	0.676
101	Ohnuki	0.1	0.051	0.3	5.882	45	0.6	0.128	0.611
102	Ohnuki	0.1	0.051	0.3	5.882	45	0.6	0.188	0.530
103	Ohnuki	0.1	0.051	0.3	5.882	45	0.6	0.235	0.496
104	Ohnuki	0.1	0.051	0.3	5.882	45	0.6	0.316	0.449
105	Ohnuki	0.1	0.076	0.4	5.263	45	0.6	0.000	0.716
106	Ohnuki	0.1	0.076	0.4	5.263	45	0.6	0.032	0.663
107	Ohnuki	0.1	0.076	0.4	5.263	45	0.6	0.081	0.634
108	Ohnuki	0.1	0.076	0.4	5.263	45	0.6	0.113	0.609
109	Ohnuki	0.1	0.076	0.4	5.263	45	0.6	0.156	0.581
110	Ohnuki	0.1	0.076	0.4	5.263	45	0.6	0.197	0.554
111	Ohnuki	0.1	0.076	0.4	5.263	45	0.6	0.226	0.524
112	Ohnuki	0.1	0.076	0.4	5.263	45	0.6	0.261	0.501
113	Ohnuki	0.1	0.076	0.4	5.263	45	0.6	0.307	0.468
114	Ohnuki	0.1	0.076	0.4	5.263	45	0.6	0.006	0.700
115	Ohnuki	0.1	0.076	0.4	5.263	45	0.6	0.037	0.690
116	Ohnuki	0.1	0.076	0.4	5.263	45	0.6	0.079	0.661
117	Ohnuki	0.1	0.076	0.4	5.263	45	0.6	0.123	0.632
118	Ohnuki	0.1	0.076	0.4	5.263	45	0.6	0.149	0.609
119	Ohnuki	0.1	0.076	0.4	5.263	45	0.6	0.192	0.576
120	Ohnuki	0.1	0.076	0.4	5.263	45	0.6	0.245	0.545

No.	Author	P [MPa]	D [m]	L [m]	L/D [m]	θ	l [m]	$j_f^{*0.5}$	$j_g^{*0.5}$
121	Ohnuki	0.1	0.076	0.4	5.263	45	0.6	0.271	0.517
122	Ohnuki	0.1	0.026	0.08	3.077	40	0.19	0.003	0.651
123	Ohnuki	0.1	0.026	0.08	3.077	40	0.19	0.106	0.562
124	Ohnuki	0.1	0.026	0.08	3.077	40	0.19	0.174	0.523
125	Ohnuki	0.1	0.026	0.08	3.077	40	0.19	0.304	0.464
126	Ohnuki	0.1	0.026	0.08	3.077	40	0.19	0.335	0.405
127	Ohnuki	0.1	0.026	0.08	3.077	40	0.19	0.521	0.332
128	Ohnuki	0.1	0.026	0.08	3.077	40	0.19	0.732	0.209
129	Ohnuki	0.1	0.026	0.19	7.308	40	0.038	0.000	0.522
130	Ohnuki	0.1	0.026	0.19	7.308	40	0.038	0.074	0.492
131	Ohnuki	0.1	0.026	0.19	7.308	40	0.038	0.113	0.442
132	Ohnuki	0.1	0.026	0.19	7.308	40	0.038	0.133	0.423
133	Ohnuki	0.1	0.026	0.19	7.308	40	0.038	0.173	0.382
134	Ohnuki	0.1	0.026	0.19	7.308	40	0.038	0.228	0.343
135	Ohnuki	0.1	0.026	0.19	7.308	40	0.038	0.264	0.310
136	Ohnuki	0.1	0.026	0.19	7.308	40	0.038	0.294	0.277
137	Ohnuki	0.1	0.026	0.19	7.308	40	0.038	0.478	0.194
138	Ohnuki	0.1	0.026	0.19	7.308	40	0.038	0.002	0.541
139	Ohnuki	0.1	0.026	0.19	7.308	40	0.038	0.066	0.483
140	Ohnuki	0.1	0.026	0.19	7.308	40	0.038	0.130	0.443
141	Ohnuki	0.1	0.026	0.19	7.308	40	0.038	0.145	0.423
142	Ohnuki	0.1	0.026	0.19	7.308	40	0.038	0.212	0.390
143	Ohnuki	0.1	0.026	0.19	7.308	40	0.038	0.247	0.343
144	Ohnuki	0.1	0.026	0.19	7.308	40	0.038	0.277	0.309
145	Ohnuki	0.1	0.026	0.19	7.308	40	0.038	0.308	0.281
146	Ohnuki	0.1	0.026	0.19	7.308	40	0.038	0.422	0.193
147	Wan		0.051	2.958	58	90		0.201	0.378
148	Wan		0.051	2.958	58	90		0.252	0.351
149	Wan		0.051	2.958	58	90		0.262	0.337
150	Wan		0.051	2.958	58	90		0.273	0.337
151	Wan		0.051	2.958	58	90		0.278	0.326
152	Wan		0.051	2.958	58	90		0.373	0.271
153	Wan		0.051	2.958	58	90		0.384	0.268
154	Wan		0.051	2.958	58	90		0.453	0.226
155	Wan		0.051	2.958	58	90		0.459	0.217
156	Wan		0.051	2.958	58	91		0.212	0.341
157	Wan		0.051	2.958	58	91		0.242	0.330
158	Wan		0.051	2.958	58	91		0.292	0.301
159	Wan		0.051	2.958	58	91		0.332	0.262
160	Wan		0.051	2.958	58	91		0.373	0.243

No.	Author	P [MPa]	D _i [m]	L [m]	L/D [m]	θ	l [m]	$J_f^{*0.5}$	$J_g^{*0.5}$
161	Wan		0.051	2.958	58	91		0.423	0.213
162	Wan		0.051	2.958	58	91		0.510	0.162
163	Wan		0.051	2.958	58	91		0.519	0.142
164	Wan		0.051	2.958	58	91		0.568	0.127
165	Siddiqui	0.1	0.038	2.36	62.1053	90		0.147	0.384
166	Siddiqui	0.1	0.038	2.36	62.1053	90		0.165	0.386
167	Siddiqui	0.1	0.038	2.36	62.1053	90		0.190	0.368
168	Siddiqui	0.1	0.038	2.36	62.1053	90		0.267	0.325
169	Siddiqui	0.1	0.038	2.36	62.1053	90		0.300	0.296
170	Siddiqui	0.1	0.038	2.36	62.1053	90		0.342	0.280
171	Siddiqui	0.1	0.038	2.36	62.1053	90		0.355	0.255
172	Siddiqui	0.1	0.044	2.24	50.9091	90		0.123	0.422
173	Siddiqui	0.1	0.044	2.24	50.9091	90		0.174	0.390
174	Siddiqui	0.1	0.044	2.24	50.9091	90		0.214	0.355
175	Siddiqui	0.1	0.044	2.24	50.9091	90		0.245	0.347
176	Siddiqui	0.1	0.044	2.24	50.9091	90		0.247	0.332
177	Siddiqui	0.1	0.044	2.24	50.9091	90		0.301	0.313
178	Siddiqui	0.1	0.044	2.24	50.9091	90		0.301	0.301
179	Siddiqui	0.1	0.044	2.24	50.9091	90		0.348	0.283
180	Siddiqui	0.1	0.044	2.24	50.9091	90		0.390	0.268
181	Siddiqui	0.1	0.044	2.24	50.9091	90		0.391	0.247
182	Siddiqui	0.1	0.044	2.24	50.9091	90		0.415	0.255
183	Siddiqui	0.1	0.044	2.24	50.9091	90		0.429	0.245
184	Siddiqui	0.1	0.044	2.24	50.9091	90		0.447	0.235
185	Siddiqui	0.1	0.044	2.1	47.7273	90		0.123	0.375
186	Siddiqui	0.1	0.044	2.1	47.7273	90		0.193	0.342
187	Siddiqui	0.1	0.044	2.1	47.7273	90		0.222	0.323
188	Siddiqui	0.1	0.044	2.1	47.7273	90		0.248	0.305
189	Siddiqui	0.1	0.044	2.1	47.7273	90		0.304	0.274
190	Siddiqui	0.1	0.047	1.82	38.7234	90		0.115	0.445
191	Siddiqui	0.1	0.047	1.82	38.7234	90		0.162	0.415
192	Siddiqui	0.1	0.047	1.82	38.7234	90		0.198	0.397
193	Siddiqui	0.1	0.047	1.82	38.7234	90		0.197	0.388
194	Siddiqui	0.1	0.047	1.82	38.7234	90		0.228	0.361
195	Siddiqui	0.1	0.047	1.82	38.7234	90		0.257	0.339
196	Siddiqui	0.1	0.047	1.82	38.7234	90		0.281	0.328
197	Kawaji	0.1	0.051	2.54	49.8039	90	1	0.216	0.386
198	Kawaji	0.1	0.051	2.54	49.8039	90	1	0.251	0.362
199	Kawaji	0.1	0.051	2.54	49.8039	90	1	0.301	0.324

No.	Author	P [MPa]	D [m]	L [m]	L/D [m]	θ	l [m]	$j_f^{*0.5}$	$j_g^{*0.5}$
201	Kawaji	0.1	0.051	2.54	49.8039	90	1	0.365	0.280
202	Kawaji	0.1	0.051	2.54	49.8039	90	1	0.422	0.249
203	Kawaji	0.1	0.051	2.54	49.8039	90	1	0.470	0.236
204	UPTF	1.5	0.75	7.086	9.448	50	1.186	0.025	0.642
205	UPTF	1.5	0.75	7.086	9.448	50	1.186	0.032	0.607
206	UPTF	1.5	0.75	7.086	9.448	50	1.186	0.045	0.588
207	UPTF	1.5	0.75	7.086	9.448	50	1.186	0.050	0.582
208	UPTF	1.5	0.75	7.086	9.448	50	1.186	0.072	0.569
209	UPTF	1.5	0.75	7.086	9.448	50	1.186	0.117	0.538
210	UPTF	1.5	0.75	7.086	9.448	50	1.186	0.156	0.499
211	MHYRESA	0.1	0.351	2.645	7.536	50	1.06	0.000	0.616
212	MHYRESA	0.1	0.351	2.645	7.536	50	1.06	0.024	0.602
213	MHYRESA	0.1	0.351	2.645	7.536	50	1.06	0.037	0.590
214	MHYRESA	0.1	0.351	2.645	7.536	50	1.06	0.052	0.578
215	MHYRESA	0.1	0.351	2.645	7.536	50	1.06	0.075	0.568
216	MHYRESA	0.1	0.351	2.645	7.536	50	1.06	0.101	0.554
217	MHYRESA	0.1	0.351	2.645	7.536	50	1.06	0.128	0.541
218	MHYRESA	0.1	0.351	2.645	7.536	50	1.06	0.150	0.531
219	MHYRESA	0.1	0.351	2.645	7.536	50	1.06	0.178	0.516
220	Wongwises	0.13	0.064	1.408	22	75	1.3	0.064	0.555
221	Wongwises	0.13	0.064	1.408	22	75	1.3	0.088	0.540
222	Wongwises	0.13	0.064	1.408	22	75	1.3	0.107	0.524
223	Wongwises	0.13	0.064	1.408	22	75	1.3	0.116	0.503
224	Wongwises	0.13	0.064	1.408	22	75	1.3	0.123	0.514
225	Wongwises	0.13	0.064	1.408	22	75	1.3	0.135	0.505
226	Wongwises	0.13	0.064	1.408	22	75	1.3	0.146	0.503
227	Wongwises	0.13	0.064	1.408	22	75	1.3	0.156	0.505
228	Wongwises	0.13	0.064	1.408	22	75	1.3	0.166	0.498
229	Wongwises	0.13	0.064	1.408	22	50	1.3	0.064	0.548
230	Wongwises	0.13	0.064	1.408	22	50	1.3	0.077	0.558
231	Wongwises	0.13	0.064	1.408	22	50	1.3	0.088	0.541
232	Wongwises	0.13	0.064	1.408	22	50	1.3	0.098	0.542
233	Wongwises	0.13	0.064	1.408	22	50	1.3	0.106	0.534
234	Wongwises	0.13	0.064	1.408	22	50	1.3	0.116	0.532
235	Wongwises	0.13	0.064	1.408	22	50	1.3	0.135	0.525
236	Wongwises	0.13	0.064	1.408	22	50	1.3	0.140	0.525
237	Wongwises	0.13	0.064	1.408	22	50	1.3	0.146	0.524
238	Wongwises	0.13	0.064	1.408	22	50	1.3	0.166	0.517
239	Wongwises	0.13	0.064	1.408	22	50	1.3	0.063	0.540
240	Wongwises	0.13	0.064	1.408	22	50	1.3	0.064	0.565

No.	Author	P [MPa]	D [m]	L [m]	L/D [m]	θ	l [m]	$j_f^{*0.5}$	$j_g^{*0.5}$
241	Wongwises	0.13	0.064	1.408	22	50	1.3	0.071	0.534
242	Wongwises	0.13	0.064	1.408	22	50	1.3	0.077	0.531
243	Wongwises	0.13	0.064	1.408	22	50	1.3	0.081	0.551
244	Wongwises	0.13	0.064	1.408	22	50	1.3	0.088	0.524
245	Wongwises	0.13	0.064	1.408	22	50	1.3	0.091	0.522
246	Wongwises	0.13	0.064	1.408	22	50	1.3	0.093	0.525
247	Wongwises	0.13	0.064	1.408	22	50	1.3	0.099	0.528
248	Wongwises	0.13	0.064	1.408	22	50	1.3	0.107	0.541
249	Wongwises	0.13	0.064	1.408	22	50	1.3	0.107	0.524
250	Wongwises	0.13	0.064	1.408	22	50	1.3	0.112	0.533
251	Wongwises	0.13	0.064	1.408	22	50	1.3	0.117	0.520
252	Wongwises	0.13	0.064	1.408	22	50	1.3	0.123	0.507
253	Wongwises	0.13	0.064	1.408	22	50	1.3	0.126	0.511
254	Wongwises	0.13	0.064	1.408	22	50	1.3	0.129	0.523
255	Wongwises	0.13	0.064	1.408	22	50	1.3	0.130	0.512
256	Wongwises	0.13	0.064	1.408	22	50	1.3	0.135	0.506
257	Wongwises	0.13	0.064	1.408	22	50	1.3	0.140	0.498
258	Wongwises	0.13	0.064	1.408	22	50	1.3	0.146	0.497
259	Wongwises	0.13	0.064	1.408	22	50	1.3	0.151	0.490
260	Wongwises	0.13	0.064	1.408	22	90	1.3	0.072	0.538
261	Wongwises	0.13	0.064	1.408	22	90	1.3	0.083	0.530
262	Wongwises	0.13	0.064	1.408	22	90	1.3	0.104	0.516
263	Wongwises	0.13	0.064	1.408	22	90	1.3	0.118	0.506
264	Wongwises	0.13	0.064	1.408	22	90	1.3	0.137	0.502
265	Wongwises	0.13	0.064	1.408	22	90	1.3	0.148	0.490
266	Wongwises	0.13	0.064	1.408	22	90	1.3	0.158	0.490
267	Wongwises	0.13	0.064	1.408	22	90	1.3	0.168	0.483
268	Wongwises	0.13	0.064	1.408	22	90	1.3	0.190	0.480
269	Wongwises	0.13	0.064	1.408	22	90	1.3	0.066	0.558
270	Wongwises	0.13	0.064	1.408	22	90	1.3	0.090	0.527
271	Wongwises	0.13	0.064	1.408	22	90	1.3	0.091	0.544
272	Wongwises	0.13	0.064	1.408	22	90	1.3	0.109	0.531
273	Wongwises	0.13	0.064	1.408	22	90	1.3	0.125	0.513
274	Wongwises	0.13	0.064	1.408	22	90	1.3	0.127	0.513
275	Wongwises	0.13	0.064	1.408	22	90	1.3	0.134	0.515
276	Wongwises	0.13	0.064	1.408	22	90	1.3	0.137	0.504
277	Wongwises	0.13	0.064	1.408	22	90	1.3	0.153	0.495
278	Wongwises	0.13	0.064	1.408	22	90	1.3	0.177	0.486
279	Wongwises	0.13	0.064	0.557	8.7	50	1.3	0.064	0.581
280	Wongwises	0.13	0.064	0.557	8.7	50	1.3	0.065	0.573

No.	Author	P [MPa]	D [m]	L [m]	L/D [m]	θ	l [m]	$J_f^{*0.5}$	$J_g^{*0.5}$
281	Wongwises	0.13	0.064	0.557	8.7	50	1.3	0.078	0.572
282	Wongwises	0.13	0.064	0.557	8.7	50	1.3	0.090	0.566
283	Wongwises	0.13	0.064	0.557	8.7	50	1.3	0.099	0.567
284	Wongwises	0.13	0.064	0.557	8.7	50	1.3	0.101	0.567
285	Wongwises	0.13	0.064	0.557	8.7	50	1.3	0.109	0.557
286	Wongwises	0.13	0.064	0.557	8.7	50	1.3	0.112	0.560
287	Wongwises	0.13	0.064	0.557	8.7	50	1.3	0.113	0.560
288	Wongwises	0.13	0.064	0.557	8.7	50	1.3	0.117	0.559
289	Wongwises	0.13	0.064	0.557	8.7	50	1.3	0.122	0.560
290	Wongwises	0.13	0.064	0.557	8.7	50	1.3	0.123	0.559
291	Wongwises	0.13	0.064	0.557	8.7	50	1.3	0.126	0.551
292	Wongwises	0.13	0.064	0.557	8.7	50	1.3	0.132	0.550
293	Wongwises	0.13	0.064	0.557	8.7	50	1.3	0.134	0.552
294	Wongwises	0.13	0.064	0.557	8.7	50	1.3	0.137	0.550
295	Wongwises	0.13	0.064	0.832	13	50	1.3	0.058	0.583
296	Wongwises	0.13	0.064	0.832	13	50	1.3	0.063	0.565
297	Wongwises	0.13	0.064	0.832	13	50	1.3	0.066	0.581
298	Wongwises	0.13	0.064	0.832	13	50	1.3	0.071	0.575
299	Wongwises	0.13	0.064	0.832	13	50	1.3	0.077	0.550
300	Wongwises	0.13	0.064	0.832	13	50	1.3	0.081	0.553
301	Wongwises	0.13	0.064	0.832	13	50	1.3	0.091	0.559
302	Wongwises	0.13	0.064	0.832	13	50	1.3	0.096	0.550
303	Wongwises	0.13	0.064	0.832	13	50	1.3	0.101	0.533
304	Wongwises	0.13	0.064	0.832	13	50	1.3	0.108	0.529
305	Wongwises	0.13	0.064	0.832	13	50	1.3	0.110	0.537
306	Wongwises	0.13	0.064	0.832	13	50	1.3	0.114	0.539
307	Wongwises	0.13	0.064	0.832	13	50	1.3	0.121	0.535
308	Wongwises	0.13	0.064	0.832	13	50	1.3	0.125	0.541
309	Wongwises	0.13	0.064	0.832	13	50	1.3	0.123	0.516
310	Wongwises	0.13	0.064	0.832	13	50	1.3	0.125	0.523
311	Wongwises	0.13	0.064	0.832	13	50	1.3	0.130	0.518
312	Wongwises	0.13	0.064	0.832	13	50	1.3	0.134	0.516
313	Wongwises	0.13	0.064	0.832	13	50	1.3	0.138	0.515
314	Wongwises	0.13	0.064	1.408	22	75	1.3	0.065	0.537
315	Wongwises	0.13	0.064	1.408	22	75	1.3	0.077	0.539
316	Wongwises	0.13	0.064	1.408	22	75	1.3	0.088	0.511
317	Wongwises	0.13	0.064	1.408	22	75	1.3	0.107	0.521
318	Wongwises	0.13	0.064	1.408	22	75	1.3	0.116	0.518
319	Wongwises	0.13	0.064	1.408	22	75	1.3	0.135	0.493
320	Wongwises	0.13	0.064	1.408	22	75	1.3	0.146	0.503

No.	Author	P [MPa]	D [m]	L [m]	L/D [m]	θ	l [m]	$j_f^{*0.5}$	$j_g^{*0.5}$
321	Wongwises	0.13	0.064	1.408	22	75	1.3	0.156	0.493
322	Wongwises	0.13	0.064	1.408	22	75	1.3	0.166	0.493
323	Wongwises	0.13	0.064	1.408	22	75	1.3	0.176	0.476
324	KAIST	0.1	0.08	3.388	42.35	35	0.623	0.000	0.511
325	KAIST	0.1	0.08	3.388	42.35	35	0.623	0.071	0.501
326	KAIST	0.1	0.08	3.388	42.35	35	0.623	0.106	0.487
327	KAIST	0.1	0.08	3.388	42.35	35	0.623	0.149	0.470
328	KAIST	0.1	0.08	3.388	42.35	35	0.623	0.201	0.443
329	KAIST	0.1	0.08	3.388	42.35	35	0.623	0.254	0.424
330	KAIST	0.1	0.08	3.388	42.35	35	0.623	0.302	0.416
331	KAIST	0.1	0.08	2	25	35	0.623	0.000	0.524
332	KAIST	0.1	0.08	2	25	35	0.623	0.066	0.505
333	KAIST	0.1	0.08	2	25	35	0.623	0.100	0.502
334	KAIST	0.1	0.08	2	25	35	0.623	0.151	0.476
335	KAIST	0.1	0.08	2	25	35	0.623	0.202	0.456
336	KAIST	0.1	0.08	0.928	11.6	35	0.623	0.000	0.587
337	KAIST	0.1	0.08	0.928	11.6	35	0.623	0.071	0.540
338	KAIST	0.1	0.08	0.928	11.6	35	0.623	0.104	0.527
339	KAIST	0.1	0.08	0.928	11.6	35	0.623	0.151	0.521
340	KAIST	0.1	0.08	0.49	6.125	35	0.623	0.000	0.601
341	KAIST	0.1	0.08	0.49	6.125	35	0.623	0.077	0.551
342	KAIST	0.1	0.08	0.49	6.125	35	0.623	0.109	0.540
343	KAIST	0.1	0.04	3.388	84.7	35	0.648	0.000	0.406
344	KAIST	0.1	0.04	3.388	84.7	35	0.648	0.165	0.335
345	KAIST	0.1	0.04	3.388	84.7	35	0.648	0.195	0.312
346	KAIST	0.1	0.04	3.388	84.7	35	0.648	0.255	0.312
347	KAIST	0.1	0.04	3.388	84.7	35	0.648	0.294	0.287
348	KAIST	0.1	0.04	3.388	84.7	35	0.648	0.351	0.259
349	KAIST	0.1	0.04	3.388	84.7	35	0.648	0.395	0.228
350	KAIST	0.1	0.04	1	25	35	0.648	0.000	0.549
351	KAIST	0.1	0.04	1	25	35	0.648	0.164	0.513
352	KAIST	0.1	0.04	1	25	35	0.648	0.198	0.482
353	KAIST	0.1	0.04	1	25	35	0.648	0.260	0.433
354	KAIST	0.1	0.04	1	25	35	0.648	0.286	0.433
355	KAIST	0.1	0.04	0.7	17.5	35	0.648	0.000	0.573
356	KAIST	0.1	0.04	0.7	17.5	35	0.648	0.166	0.511

BIBLIOGRAPHIC DATA SHEET

(See instructions on the reverse)

1. REPORT NUMBER
(Assigned by NRC, Add Vol., Supp., Rev.,
and Addendum Numbers, if any.)

NUREG/IA-0203

2. TITLE AND SUBTITLE

Assessment of RELAP5/MOD3.2.2 Against Flooding Database in
Horizontal-to-Inclined Pipes

3. DATE REPORT PUBLISHED

MONTH	YEAR
July	2001

4. FIN OR GRANT NUMBER

5. AUTHOR(S)

H.T. Kim, H.C. No, KAIST
S.J. Ha, N.S. Ahn, KEPRI
Y.S. Bang, KINS

6. TYPE OF REPORT

Technical

7. PERIOD COVERED (Inclusive Dates)

8. PERFORMING ORGANIZATION - NAME AND ADDRESS (If NRC, provide Division, Office or Region, U.S. Nuclear Regulatory Commission, and mailing address; if contractor, provide name and mailing address.)

Korea Advanced Institute of Science and Technology, 373-1, Gusung-Dong, Yusung-Ku, Taejon 305-701 Korea
Korea Electric Power Research Institute, 103-16 Munji-Dong, Yusung-Ku, Taejon 305-380 Korea
Korea Institute of Nuclear Safety, PO Box 114, Yuseong-Gu, Taejon 305-600 Korea

9. SPONSORING ORGANIZATION - NAME AND ADDRESS (If NRC, type "Same as above"; if contractor, provide NRC Division, Office or Region, U.S. Nuclear Regulatory Commission, and mailing address.)

Division of System Analysis and Regulatory Effectiveness
Office of Nuclear Regulatory Research
U.S. Nuclear Regulatory Commission
Washington, DC 20555-0001

10. SUPPLEMENTARY NOTES

11. ABSTRACT (200 words or less)

A total of 356 experimental data for the onset of flooding are compiled for the data bank and used for the assessment of RELAP5/MOD3.2.2 predictions of Counter-Current Flow Limitation (CCFL) in horizontal-to-inclined pipes simulating a PWR hot leg. RELAP5 calculations show that higher gas flow rates are required to initiate the flooding compared with the experimental data if the L/D is low as that of the hot legs of typical PWRs. Based on the present data bank, the new CCFL correlation is derived, which shows the L/D effect. The present correlation agrees well with the database within the prediction error, 8.7% and it is implemented into the RELAP5 and validation against the data bank. The predictions of the flooding limit by the modified version lie well on the applied CCFL curve even if the predictions by standard RELAP5 are lower than the present CCFL curve.

12. KEY WORDS/DESCRIPTORS (List words or phrases that will assist researchers in locating the report.)

RELAP5
Flooding
CCFL

13 AVAILABILITY STATEMENT

unlimited

14 SECURITY CLASSIFICATION

(This Page)

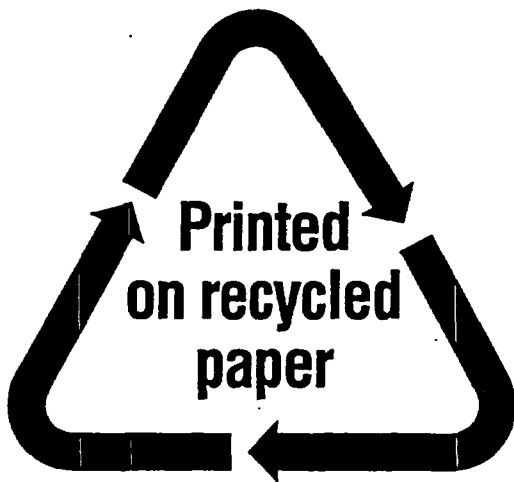
unclassified

(This Report)

unclassified

15. NUMBER OF PAGES

16. PRICE



Federal Recycling Program



UNITED STATES
NUCLEAR REGULATORY COMMISSION
WASHINGTON, DC 20555-0001

OFFICIAL BUSINESS
PENALTY FOR PRIVATE USE, \$300